# Coronal mass ejections and the solar wind

**Lucie Green**
**Mullard Space Science Laboratory, UCL**

# Aims of today's lecture

By the end of today's lecture:

- be familiar with observation methods and general properties of CMEs
- be familiar with CME models
- understand the difference between ideal and non-ideal CME models
- be familiar with open research questions in relation to CMEs
- be familiar with the history and main theoretical developments in relation to the solar wind

*But many things are missed out due to time!*
*The Living Reviews in Solar Physics are a great resource.*

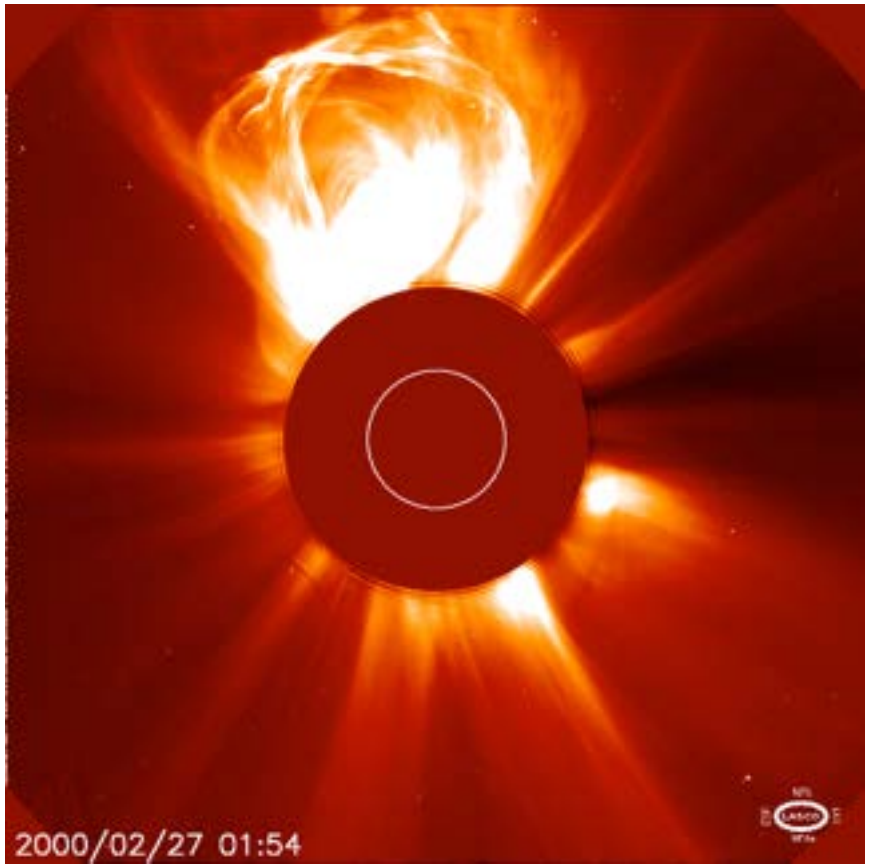


# Coronal mass ejection (CME) observations

# Coronal mass ejections

Lasco C2: 1.7 $R_{sun}$ to 6 $R_{sun}$

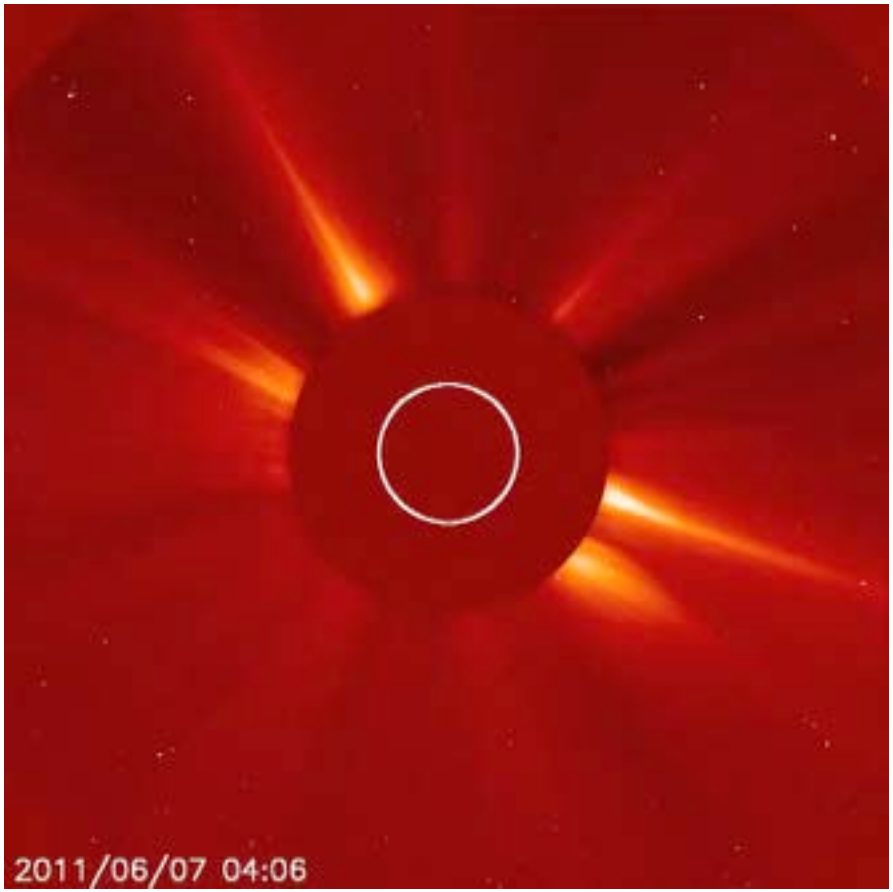


Lasco C3: 3.7 $R_{sun}$ to 32 $R_{sun}$

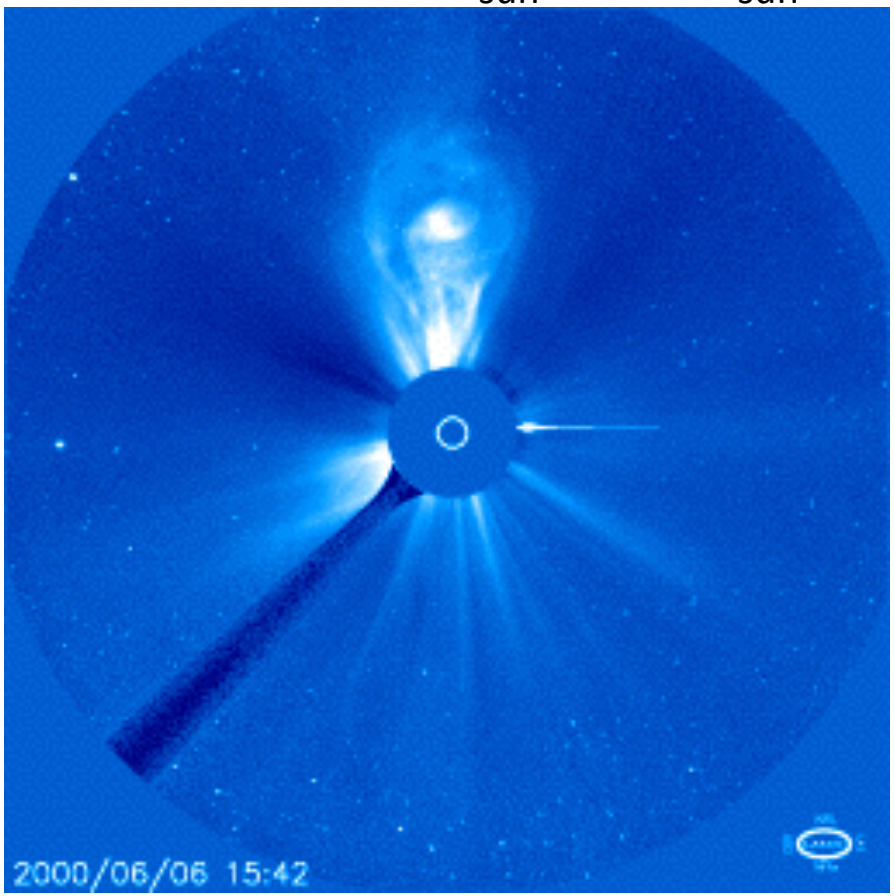


CMEs are the most energetic activity events in the Solar System, expelling ~$10^{11}$ to $10^{13}$ kg plasma at speeds of several hundred or even thousands of $kms^{-1}$

# 3-part structure

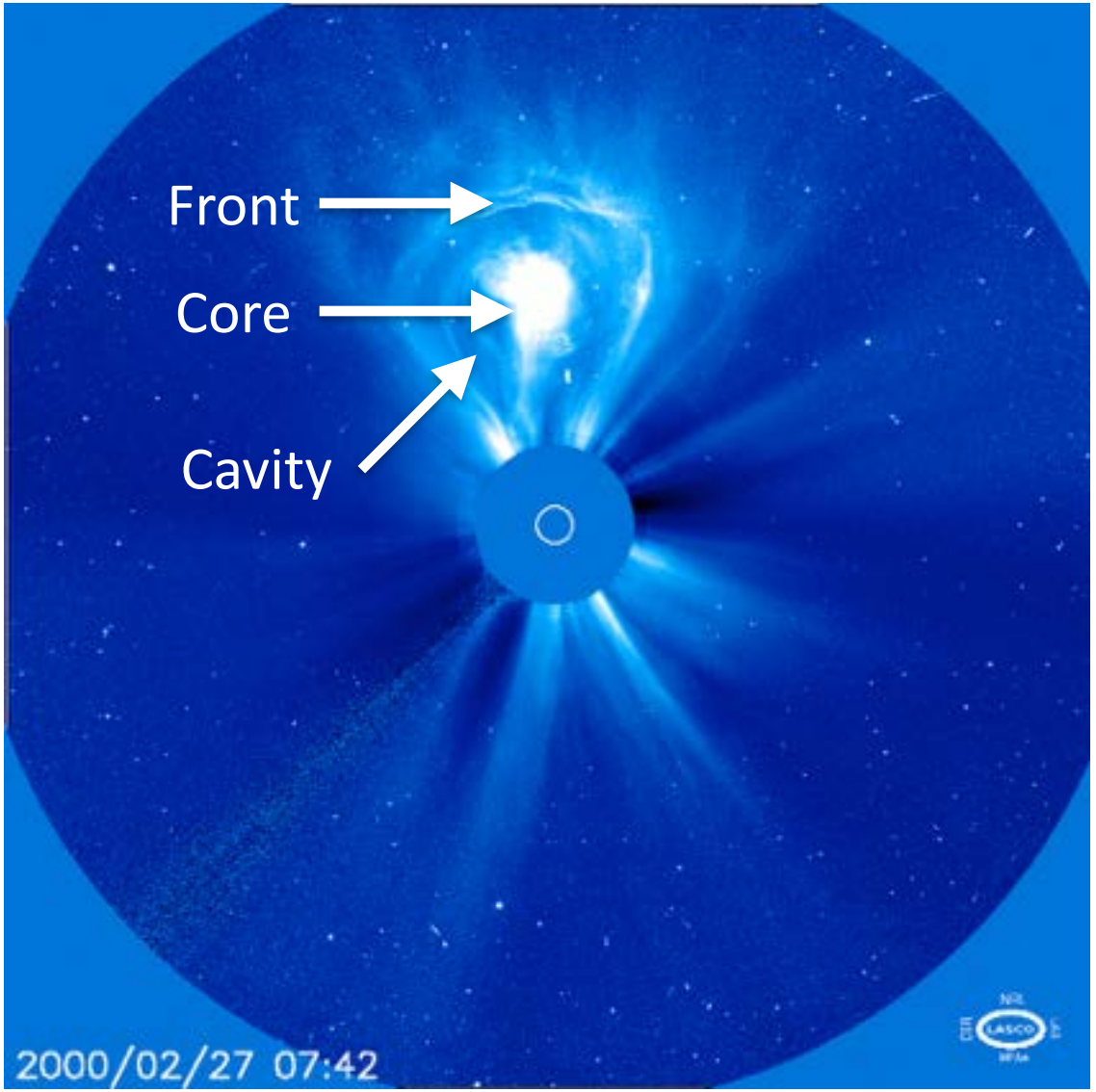

# Three-part structure

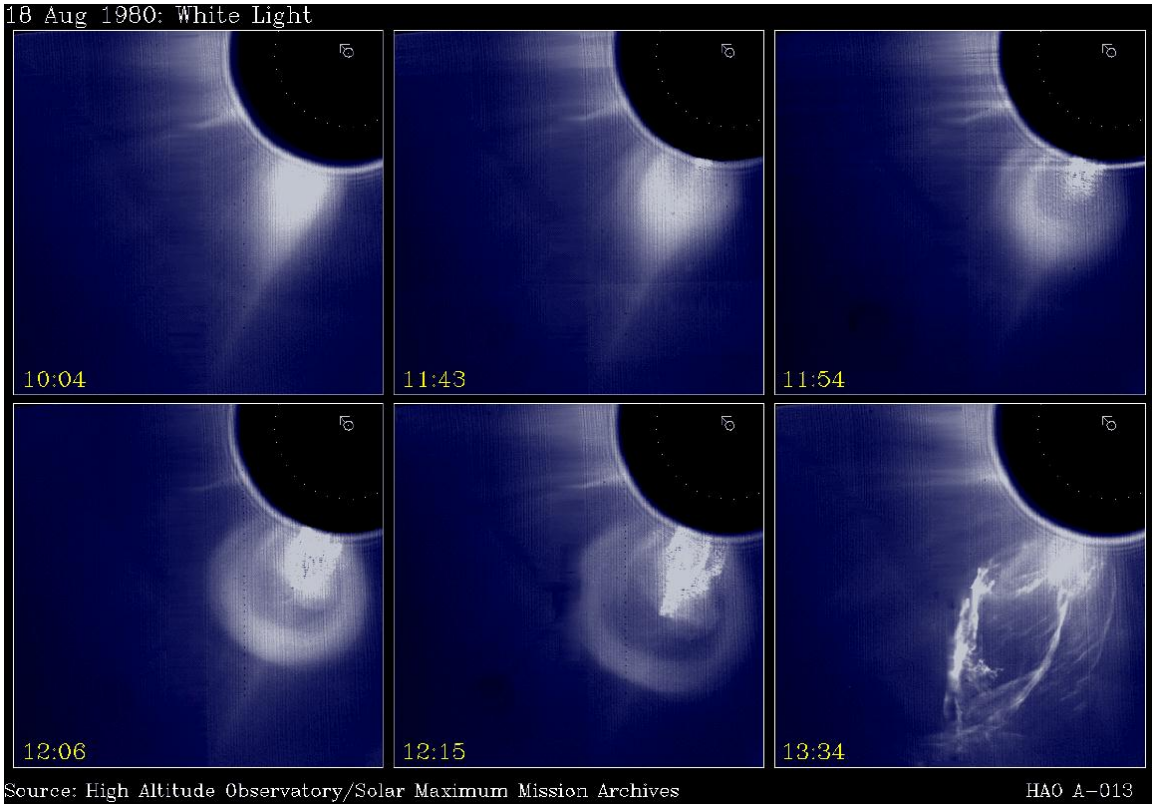


- Frontal structure (high density, coronal temperature, 'high' magnetic field strength) ~2MK, $10^{-4}$ T
- Cavity (low $n_e$, coronal T), ~2MK, few $10^{-4}$ T
- Prominence core (highest density, lowest temp., highest field strength), ~80000K, few $10^{-3}$ T

# STEREO view of CMEs

Positions in
February 2010

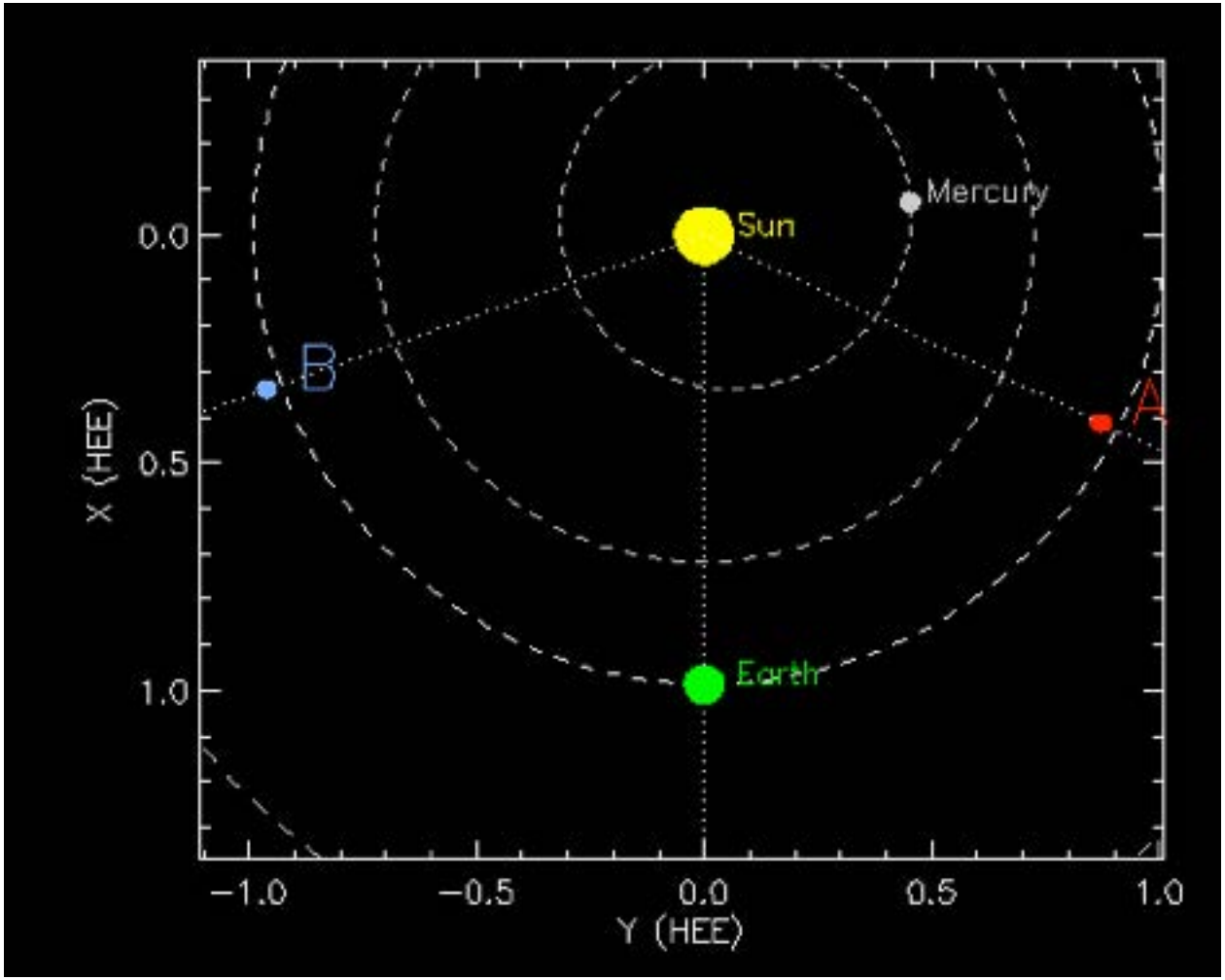


https://stereo-ssc.nascom.nasa.gov/cgi-bin/make_where_gif

# STEREO view of CMEs

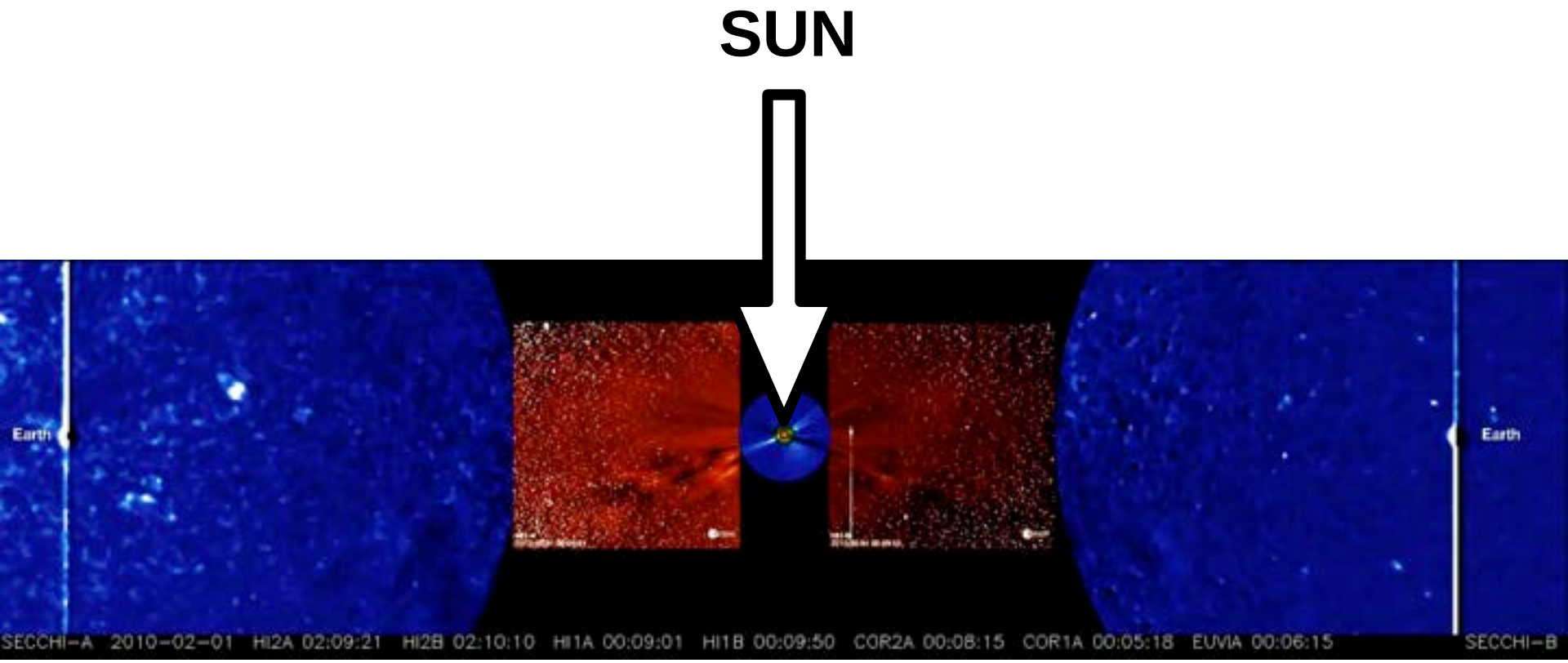

# CME properties

- Large-scale structures carrying **plasma** and **magnetic field**
- **Typical mass:** $10^{13}$ kg
- **Speed:** huge range from <200 to >2000km/s
- **Energy:** $10^{25}$ J (comparable to flares)
- **Plasma temperature:** 80,000 K (core) to 2MK (front)
- **Typical angular width:** from $70^{o}$ to $360^{o}$ ("halo" CMEs; real angular width is smaller, the halo is due to a projection effect)
- **Frequency:** one every ~5 days at cycle minimum, a few per day at cycle maximum
- **Related to:** filament eruptions, flares, shocks
- **Mass flow rate:** ~$10^{8}$ kg/s.
- CMEs contribute to the solar wind flow and the magnetic field in interplanetary space

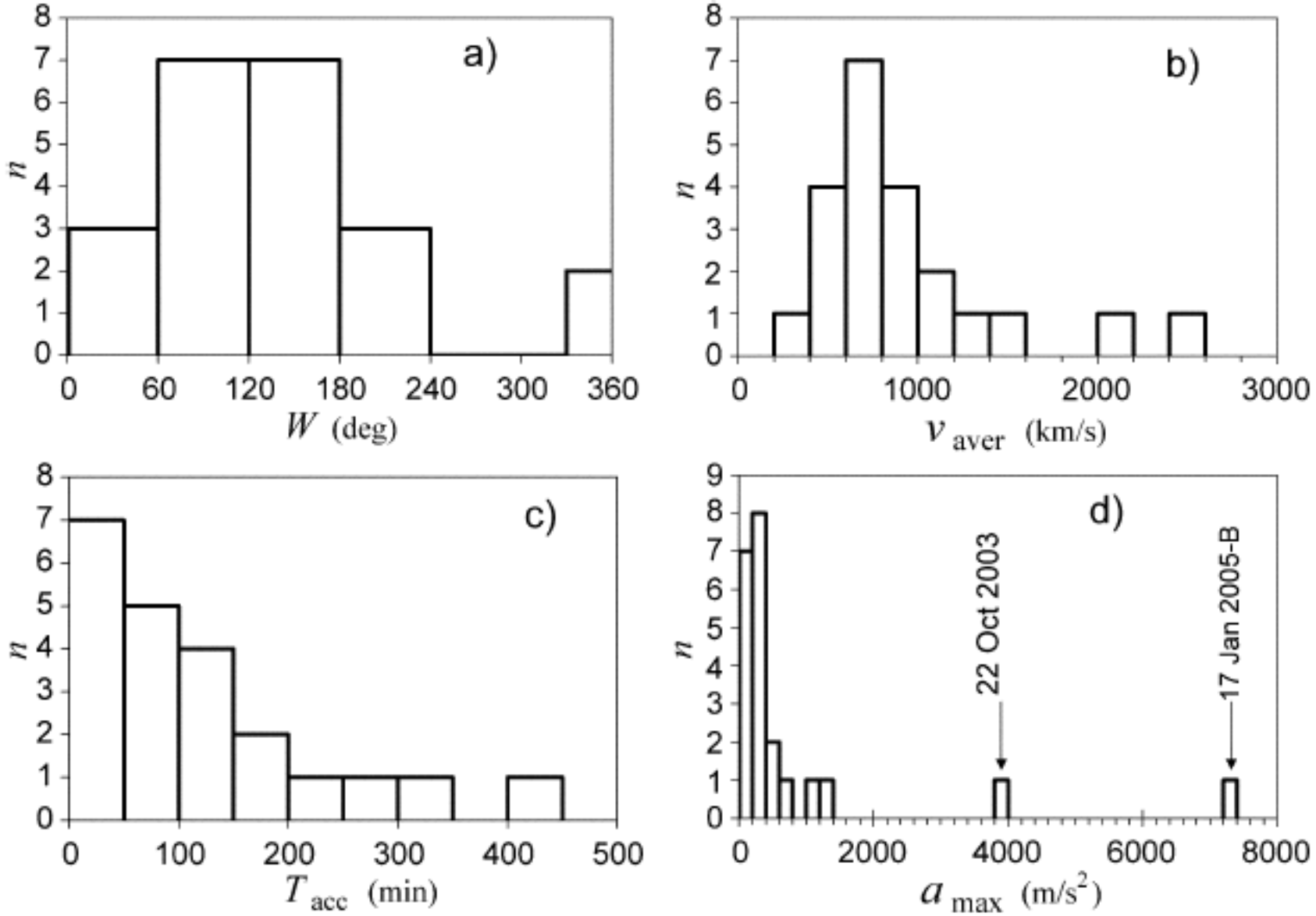


Vrsnak et al, 2007, Fig 3

# Accelerated particles

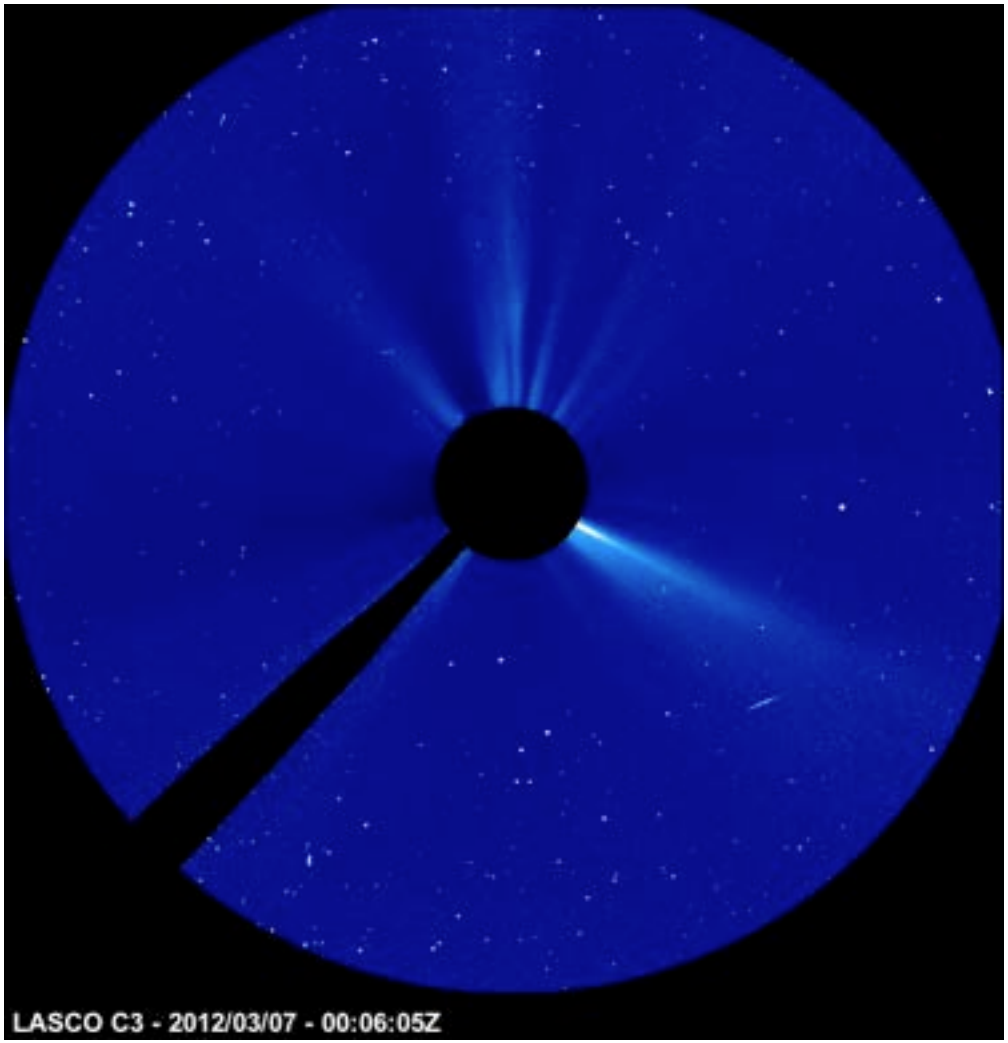

# Accelerated particles

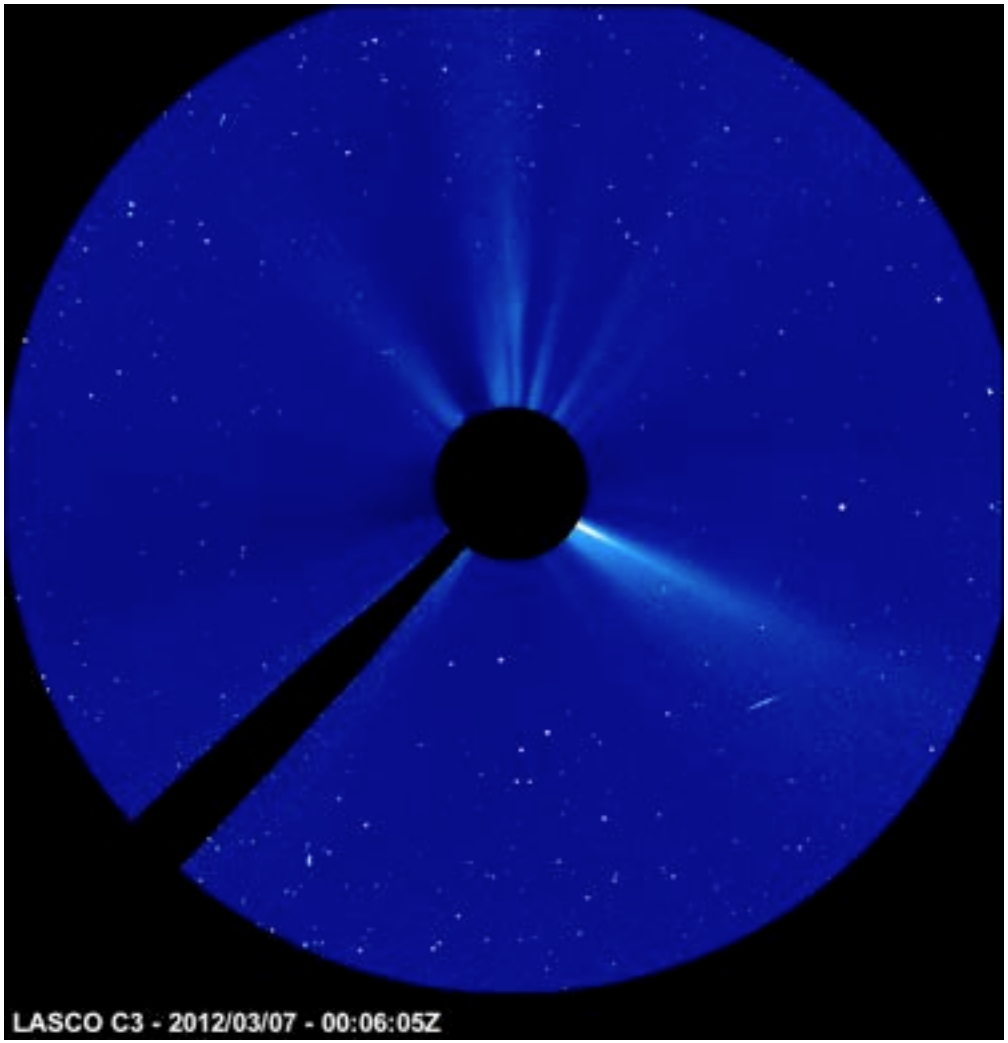

# CME observations

- CMEs are most easily seen in **white-light** with space-borne coronagraphs: they show up as bright bubble-like features moving away from the Sun
- The white-light emission is due to **Thomson scattering** (of the photospheric light by coronal electrons) therefore white-light brightness is proportional to electron density
- But coronagraphs are not the ideal way to determine CME origins - they view only > 0.1 $R_s$ in the plane-of-the-sky so the lower atmosphere is completely obscured.
- A CME launch-time can be determined by back extrapolation
- CME source regions can be studied in EUV and soft X-ray solar images.

# Measuring CME speed and onset time

CME onset time determined by repeatedly measuring height of a feature as it propagates out, then extrapolating back to the solar surface to determine the launch time.

Not an accurate process, since the eruption accelerates in the lower corona!

For movies and detailed measurements of CMEs observed with SOHO since 1996 see: http://cdaw.gsfc.nasa.gov/CME_list/

To determine onset time more accurately we can look for lower coronal CME signatures.

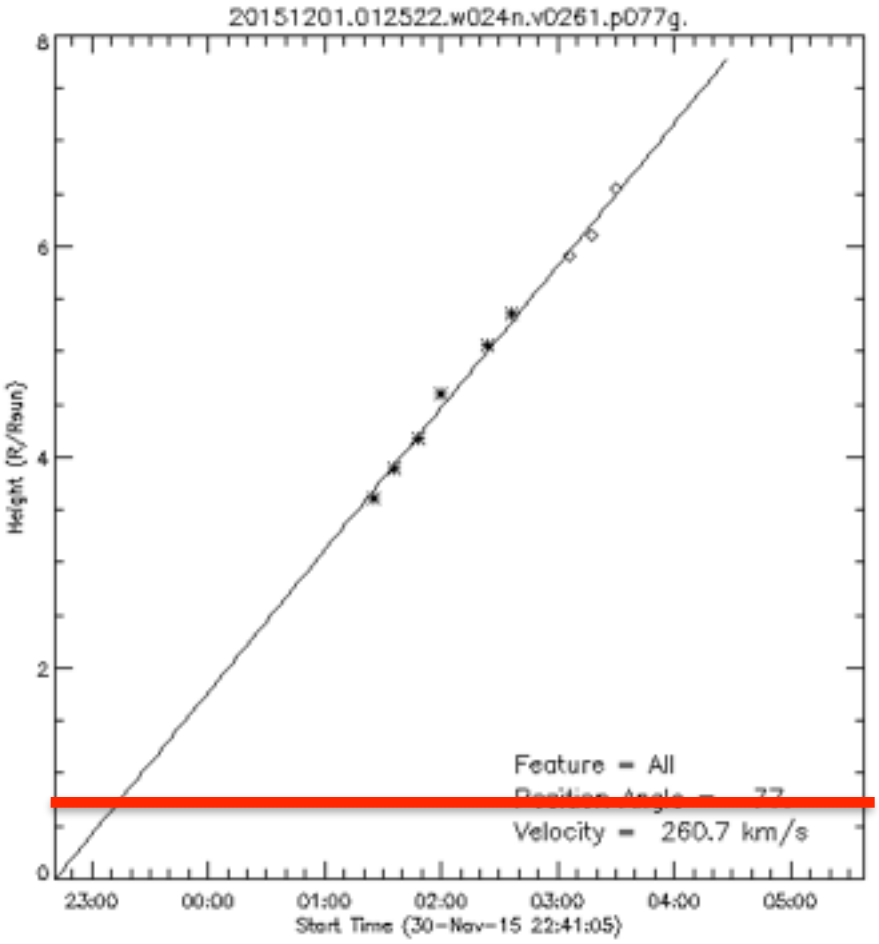

# Below the occulting disk

- CMEs are initiated in a region of the atmosphere which is dominated by magnetic field

- i.e. plasma β << 1

(i.e. above the photosphere but below 1.5 solar radii)

- But the magnetic field is rooted in the photosphere where plasma β > 1

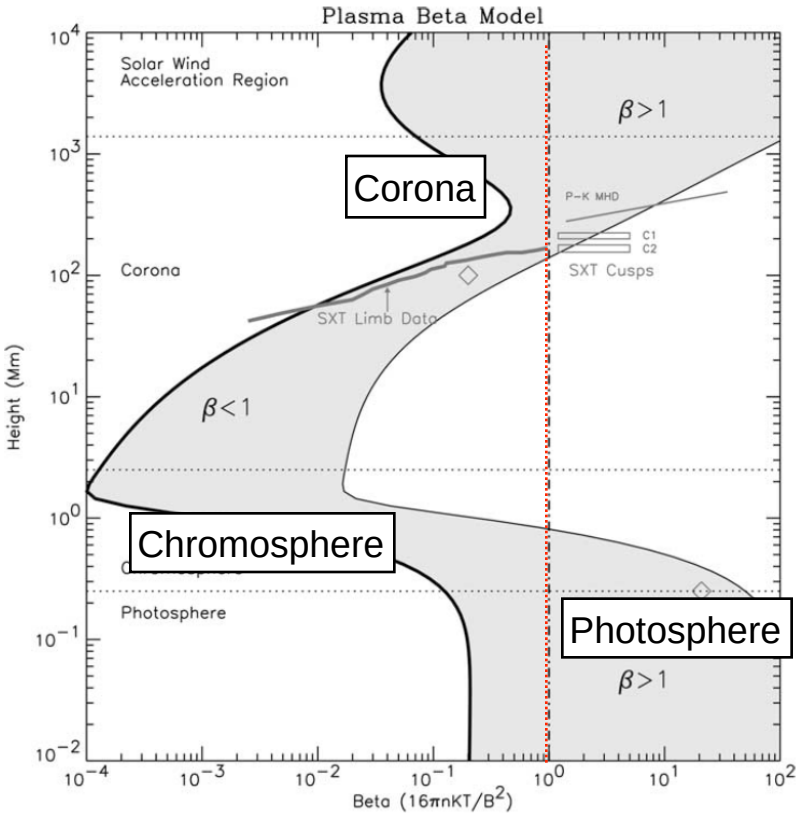


Figure from Gary, 2001

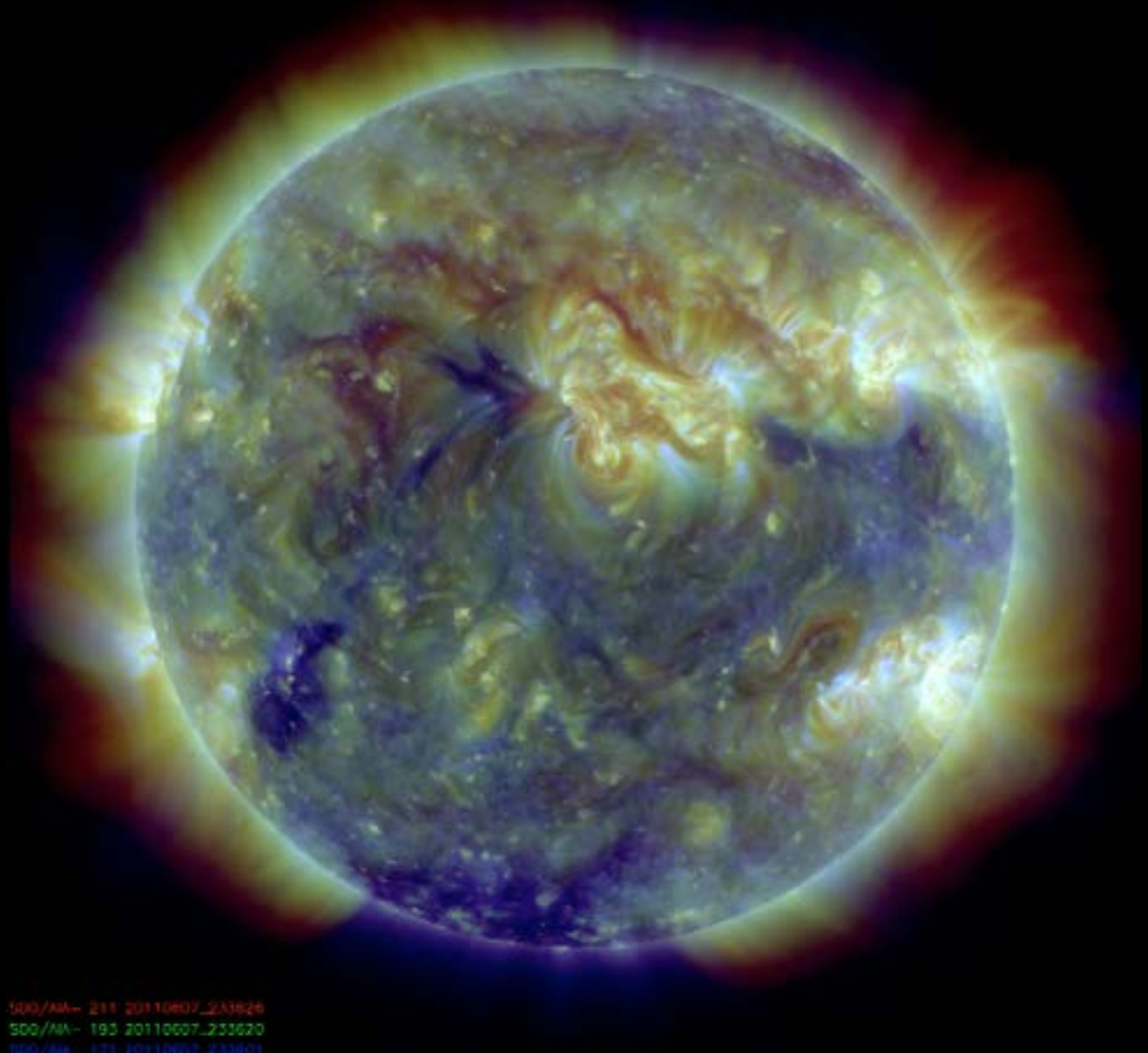
SDO/AIA - 211 20110607_233626
SDO/AIA - 193 20110607_233620
SDO/AIA - 171 20110607_233601

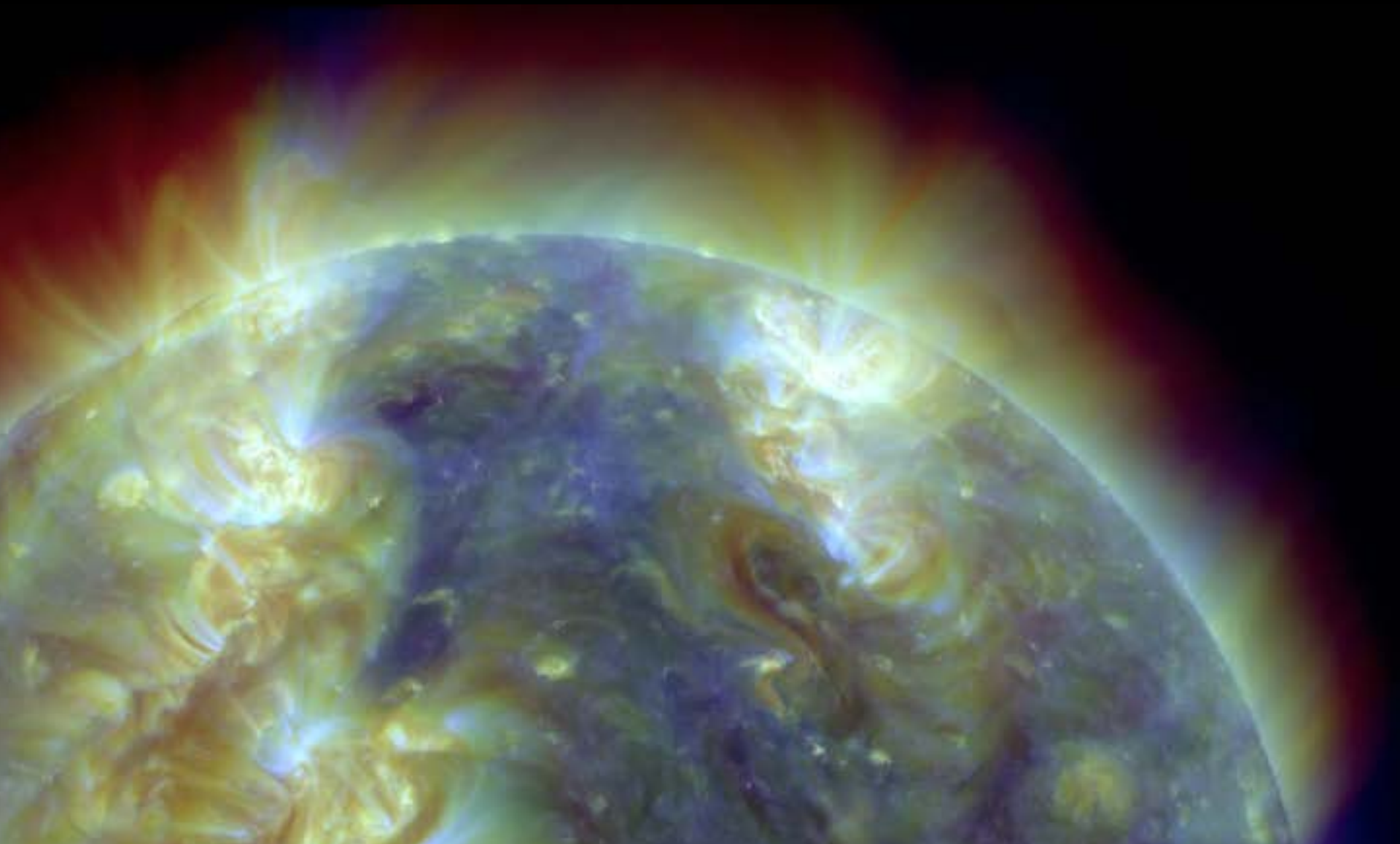

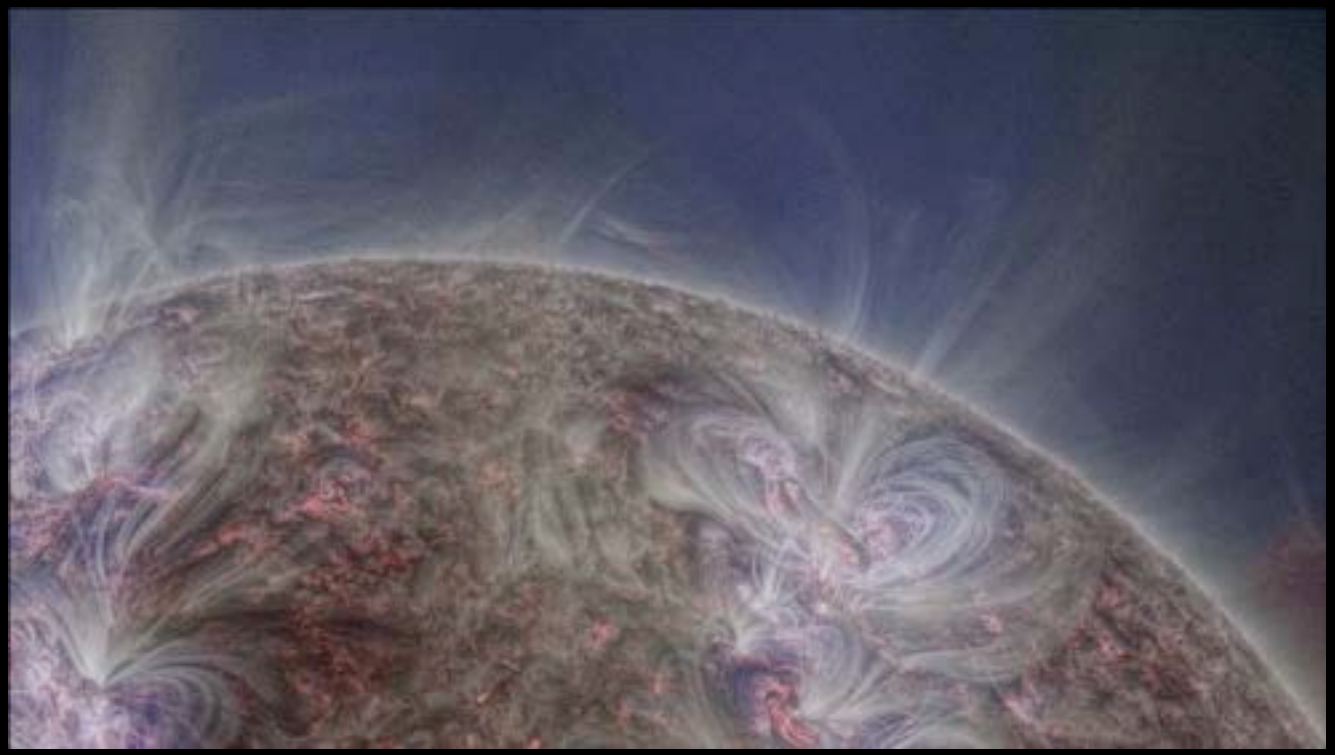

Movie courtesy of Miloslav Druckmüller

# CME initiation heights

Patsourakos, Vourlidas, Stenborg (2013)

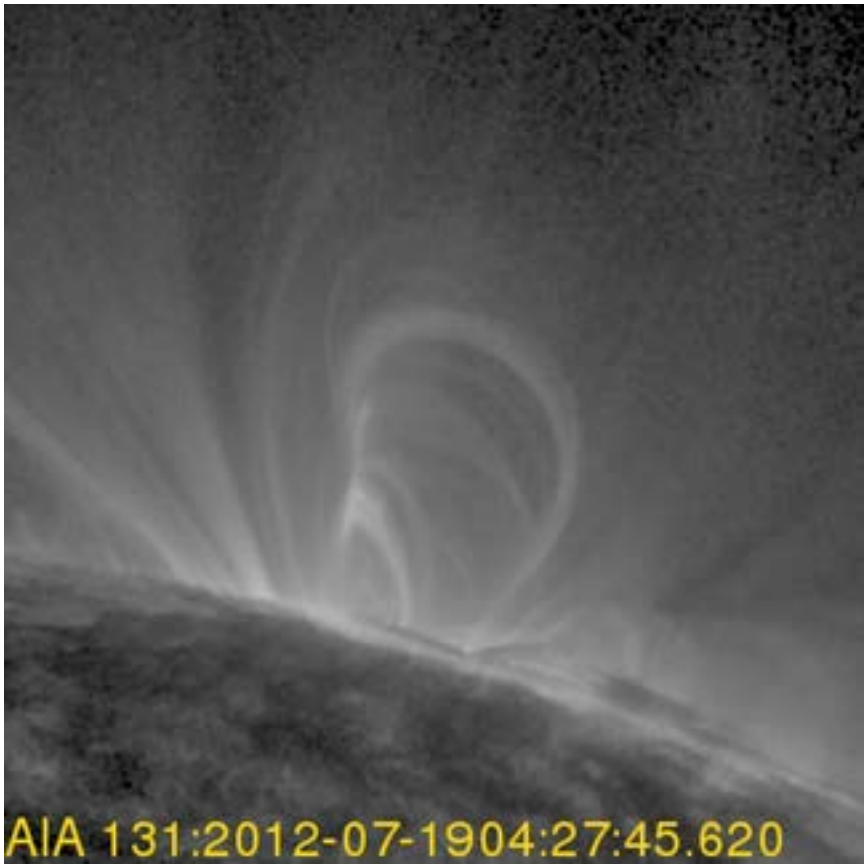

# Coronal field is driven by photospheric flows

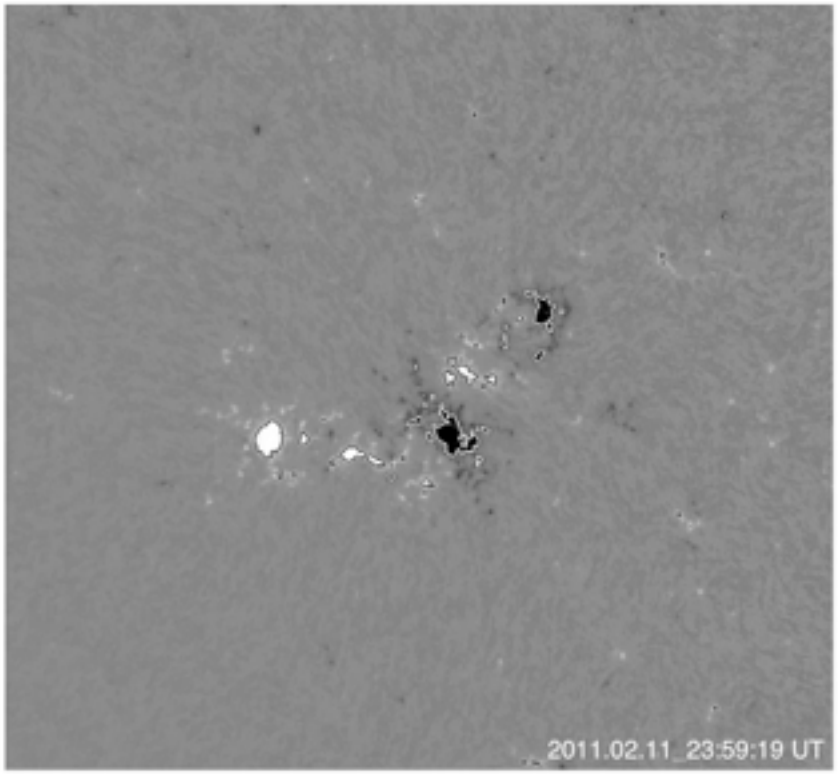


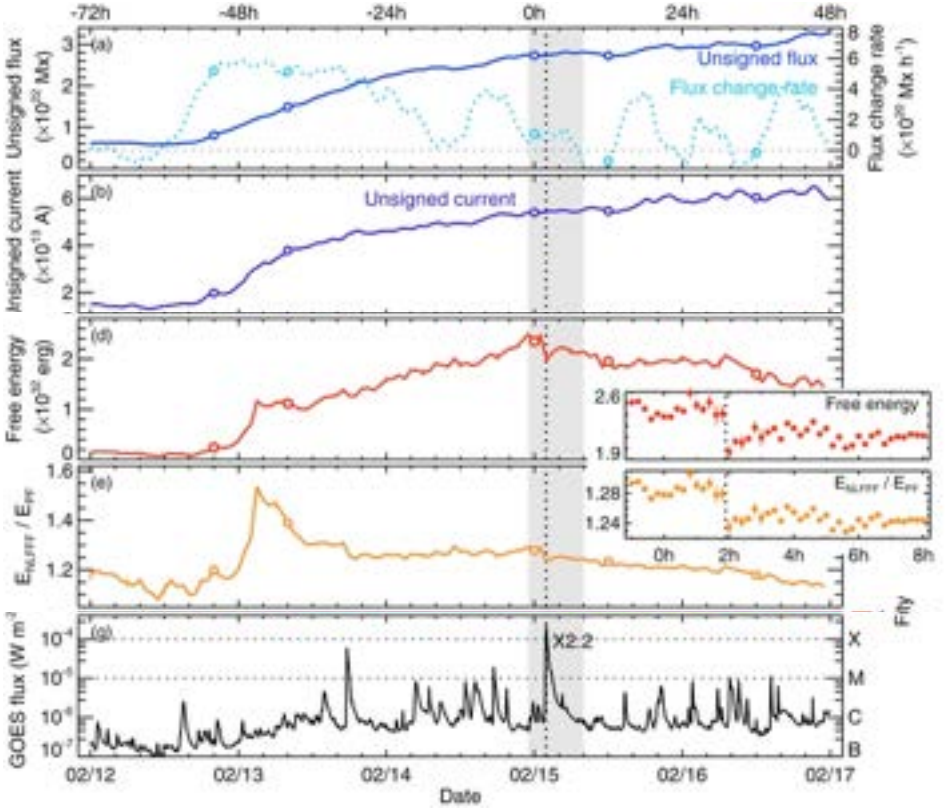


Figure from Sun et al., 2012

# Lower atmospheric signatures: filament eruptions

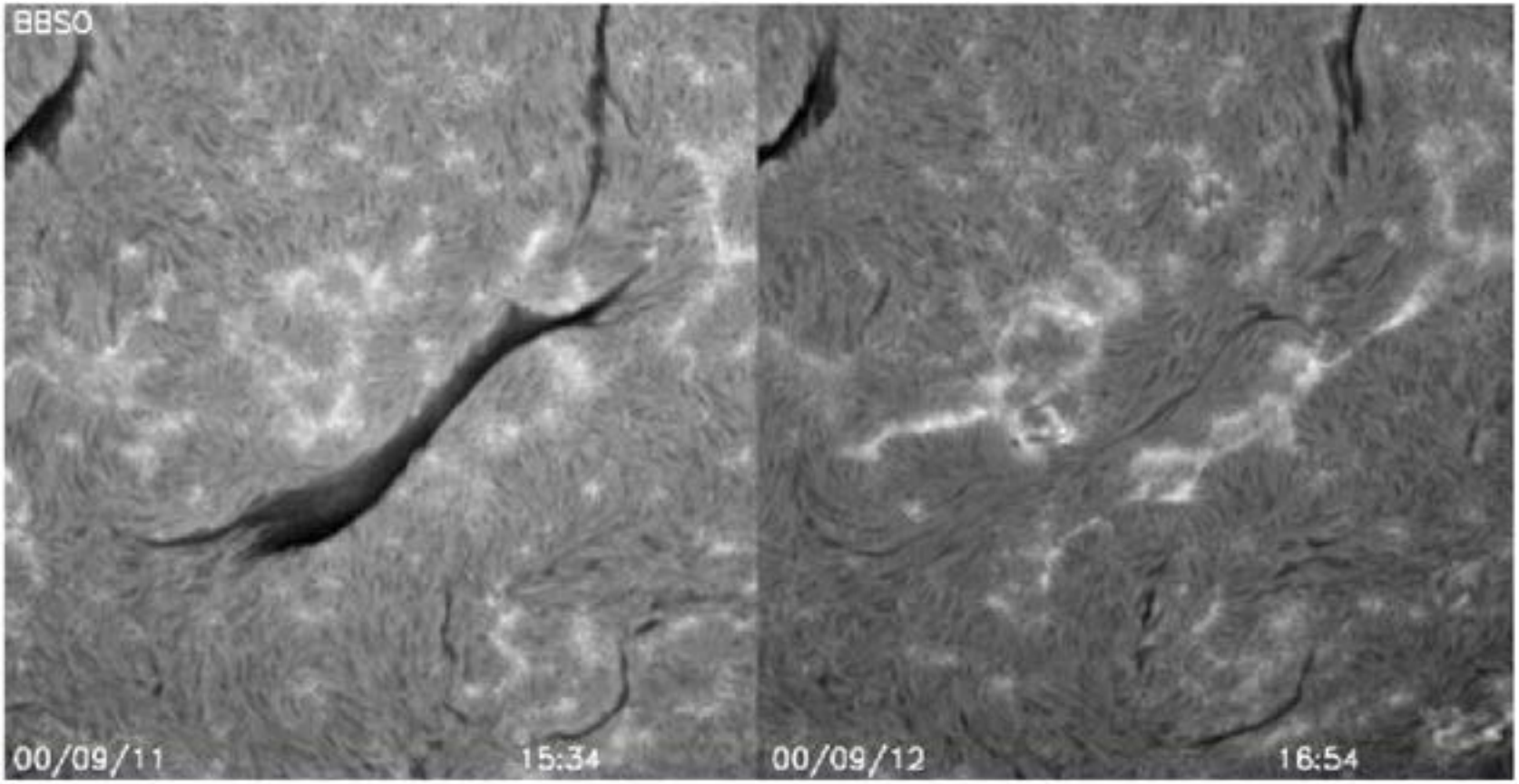


Hα filament disappears (erupts)

Two-ribbon flare structure forms after the disappearance

# Lower atmospheric signatures: filament eruptions

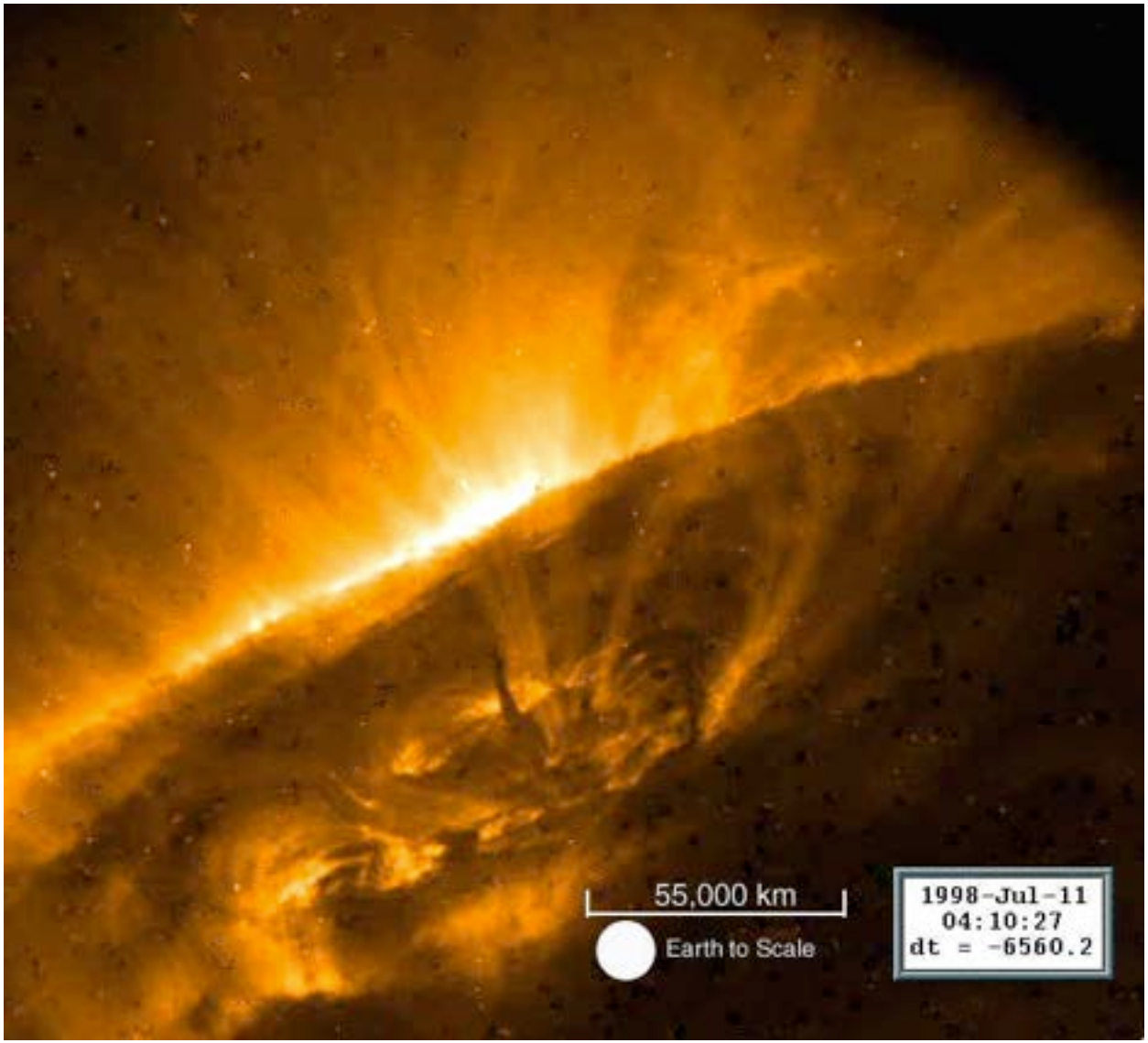

# Lower atmospheric signatures: flares

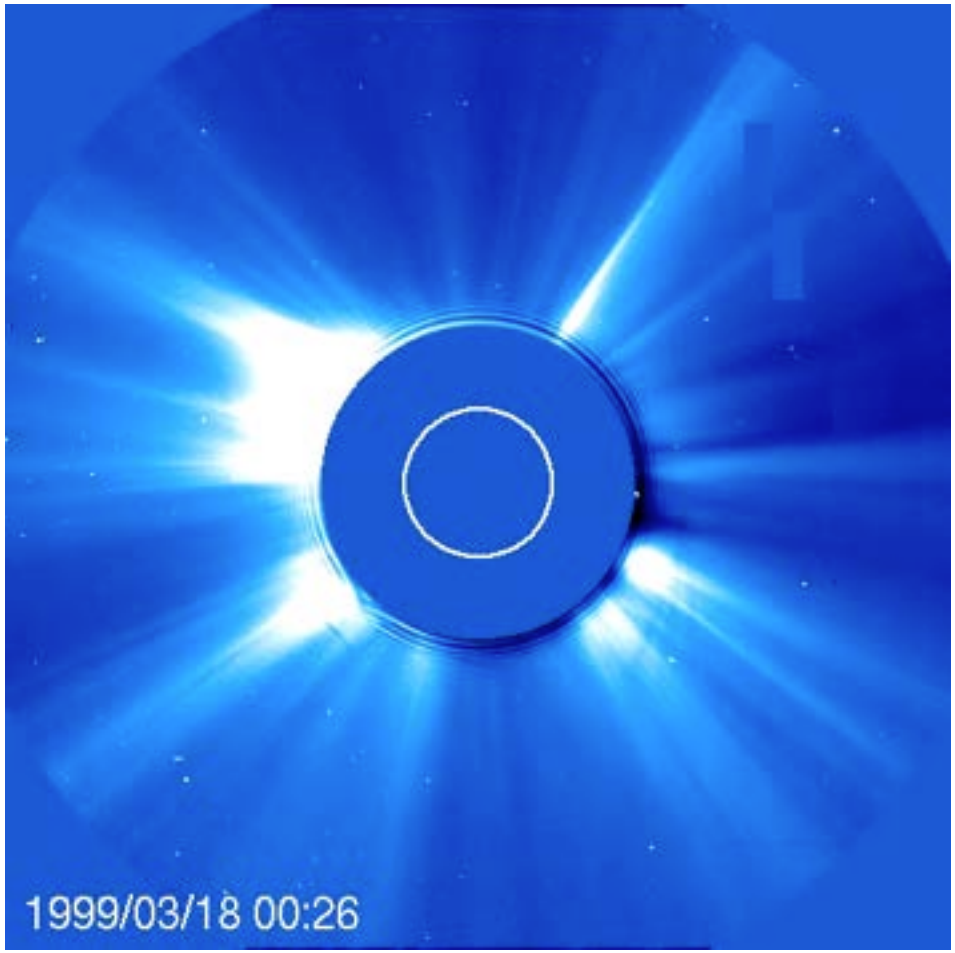


# Lower atmospheric signatures: flares

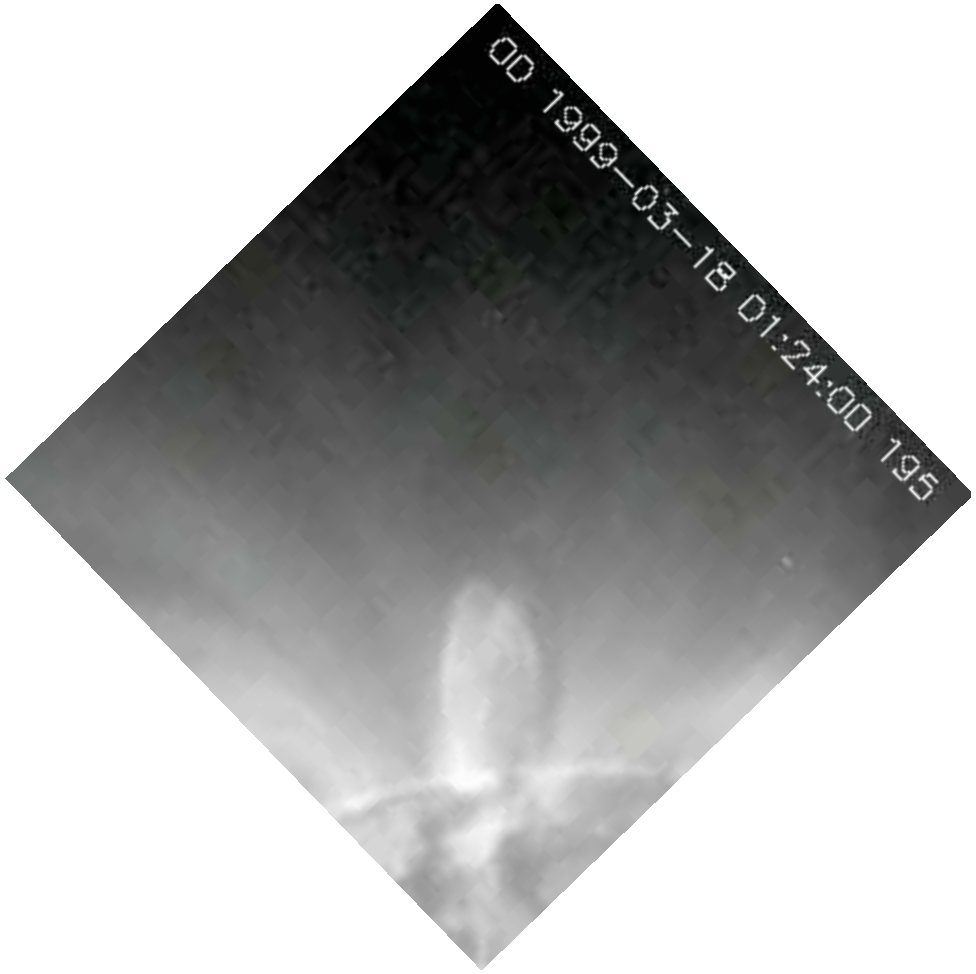


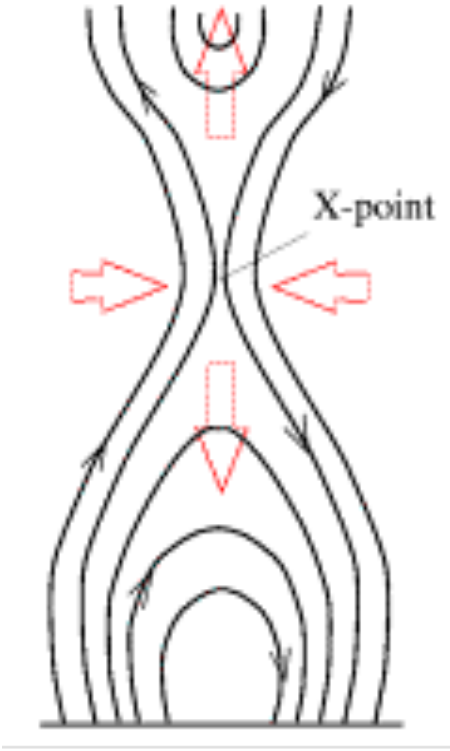

# *Magnetic reconnection*

Reconnection occurs when the diffusion term in the induction equation dominates and results in a change of magnetic field “topology”, converting magnetic energy into heat and kinetic energy.

It occurs when oppositely directed field lines approach one another.

As field is advected by a flow, it generates steep gradients - current sheets

The reconfiguration of the coronal field that reconnection produces liberates stored magnetic energy

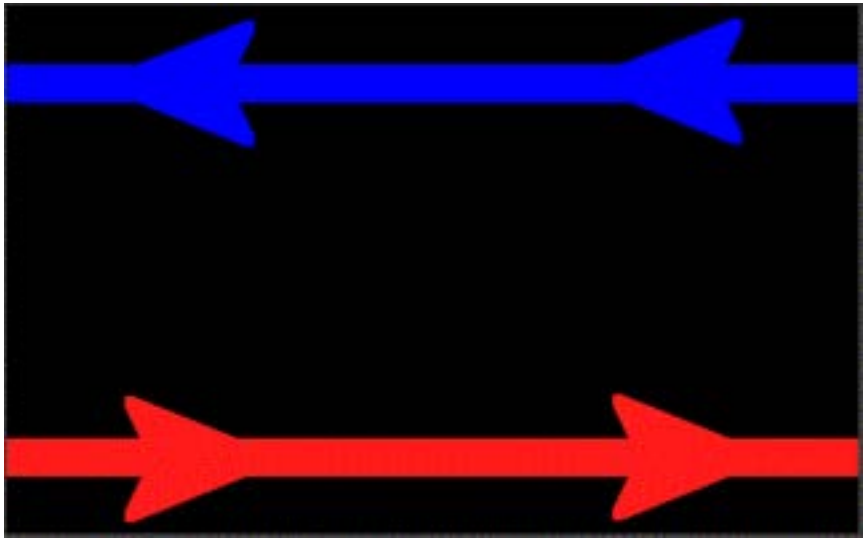

# Lower atmospheric signatures: flares

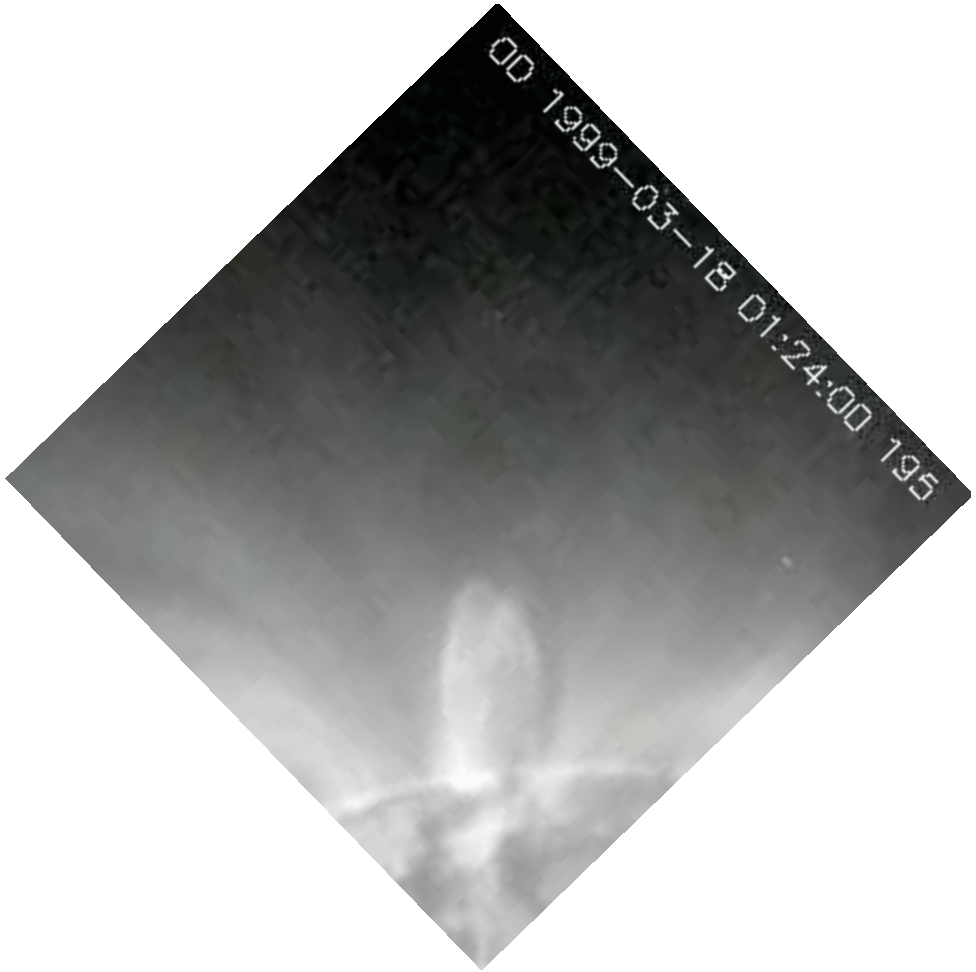


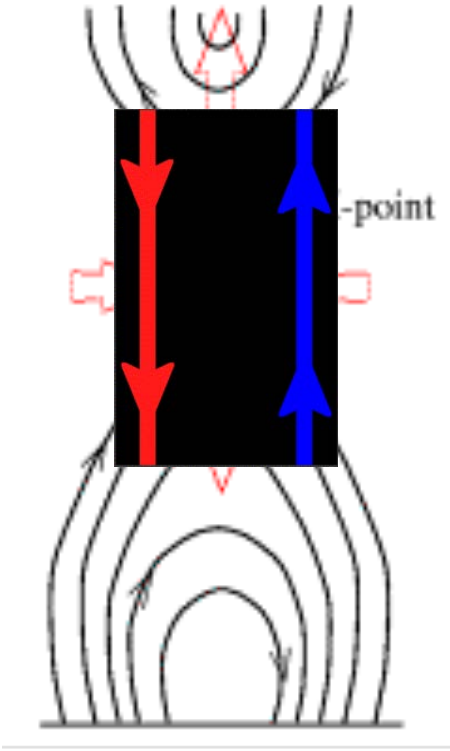

# Lower atmospheric signatures: flare loops and/or “cusps”

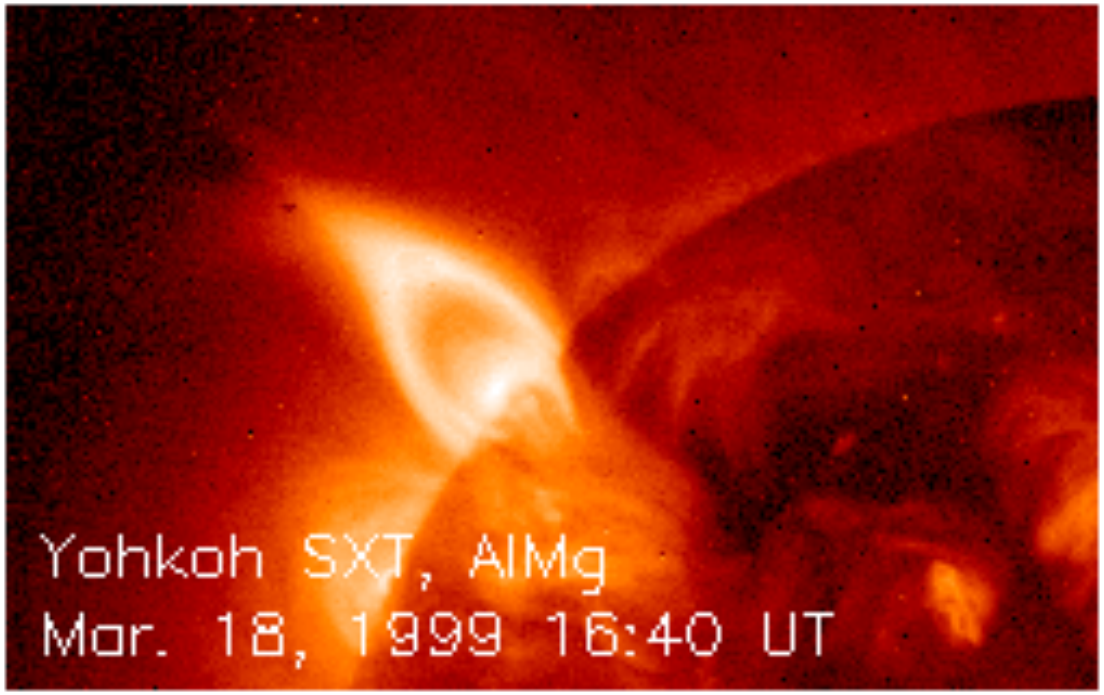


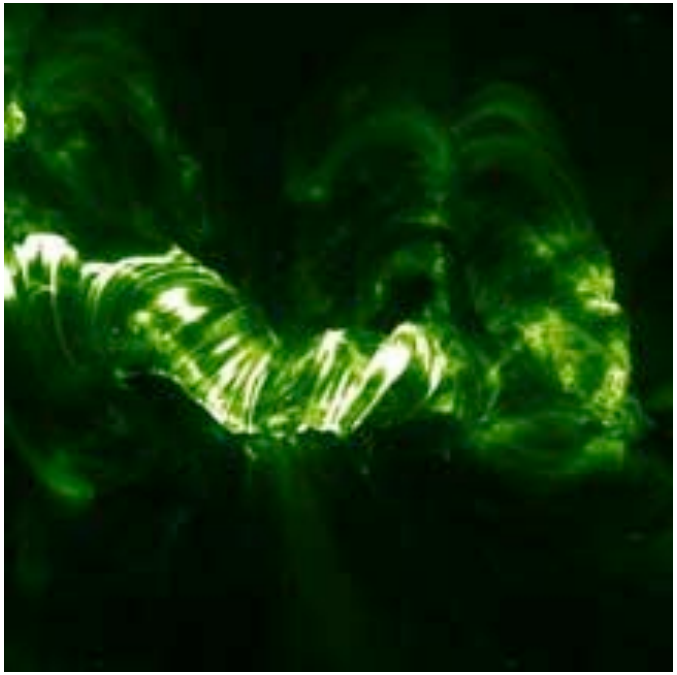

# The “standard” model

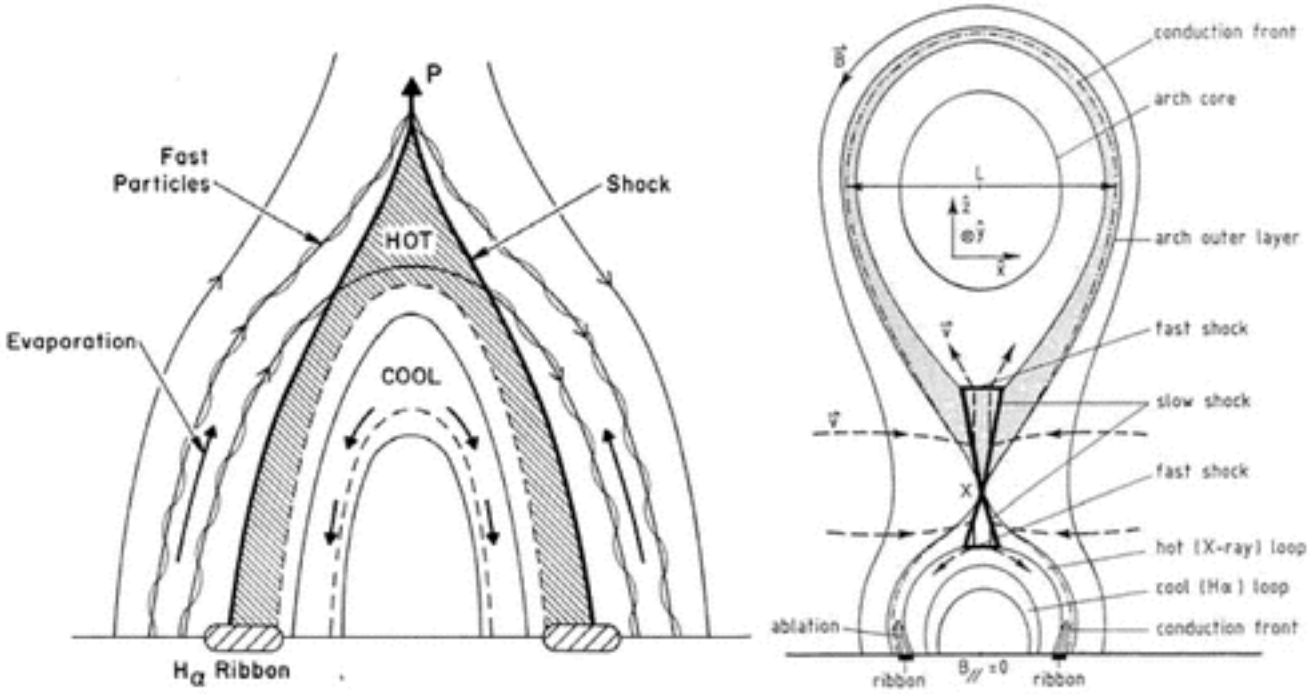


Figure 16.1: *Left:* slow-shock heating in the downward-directed reconnection outflows. The reconnection point P is rising vertically, trailing behind two slow MHD shocks (thick lines). Behind the shock there is a series of loops with heated plasma (shaded), while the cooled plasma in the inner loops falls down as seen in H$\alpha$ (Cargill & Priest 1983). *Right:* slow-shock heating in upward-directed reconnection outflows. The heated plasma connected with the slow MHD shocks forms a bubble-like conduction front of a postflare arch (Hick & Priest 1989).

Physics of the solar corona (Aschwanden)

# Standard flare-CME model

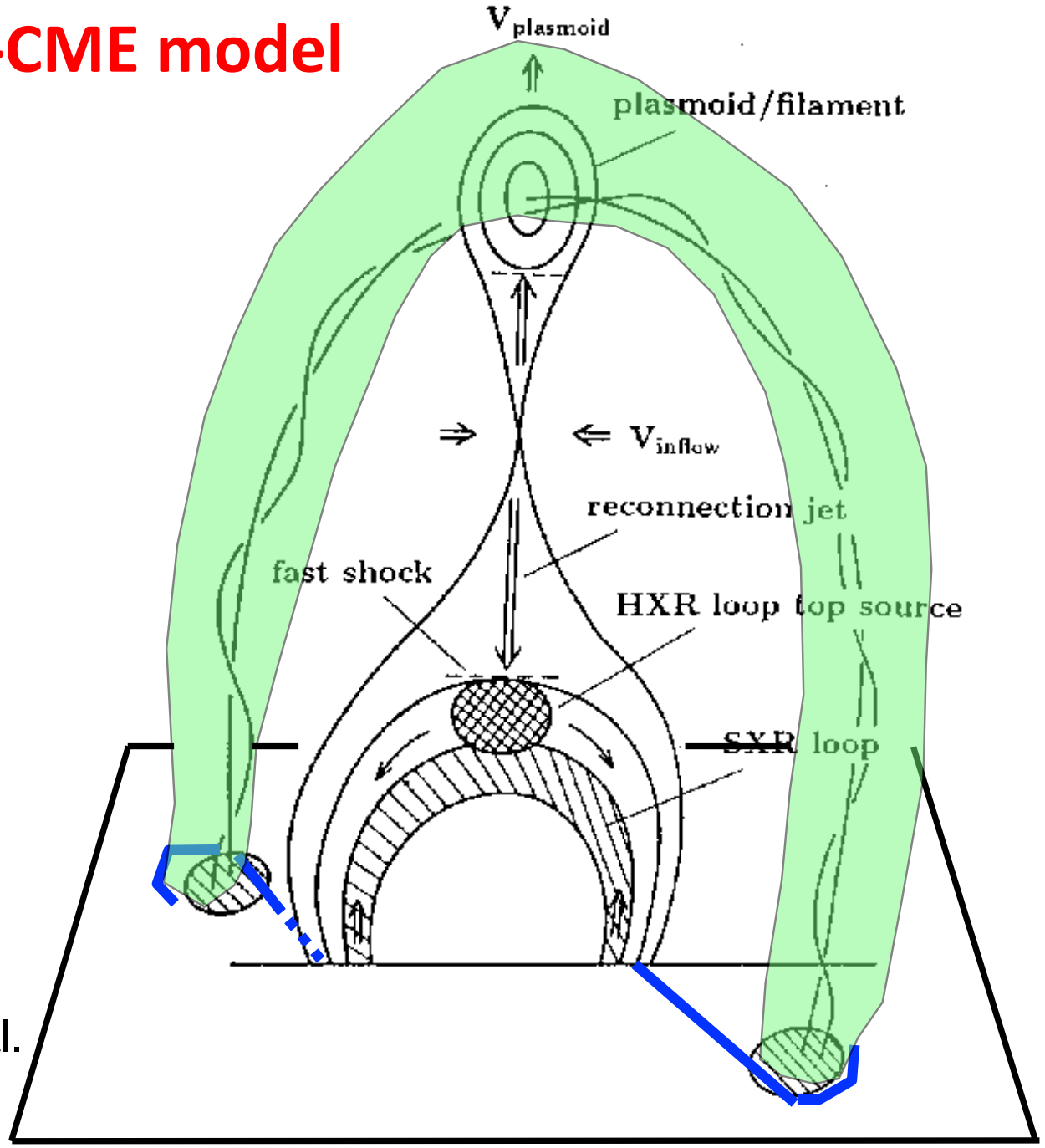


Figure 1 from Shibata et al. (1995)

# Standard flare-CME model

(1) Filament (flux rope) becomes unstable and rises (CME).

(2) Surrounding arcade of loops carried with the rising flux rope get extended (stretched).

(3) Current sheet forms under the rising flux rope, where magnetic reconnection takes place

(4) Dimmings are seen at the footpoints of the rising & expanding magnetic field.

(5)New loops are formed, channeling accelerated particles which impact the chromosphere leading to evaporation, which fills the loops with hot plasma -> flare loops  flare ribbons at the footpoints.

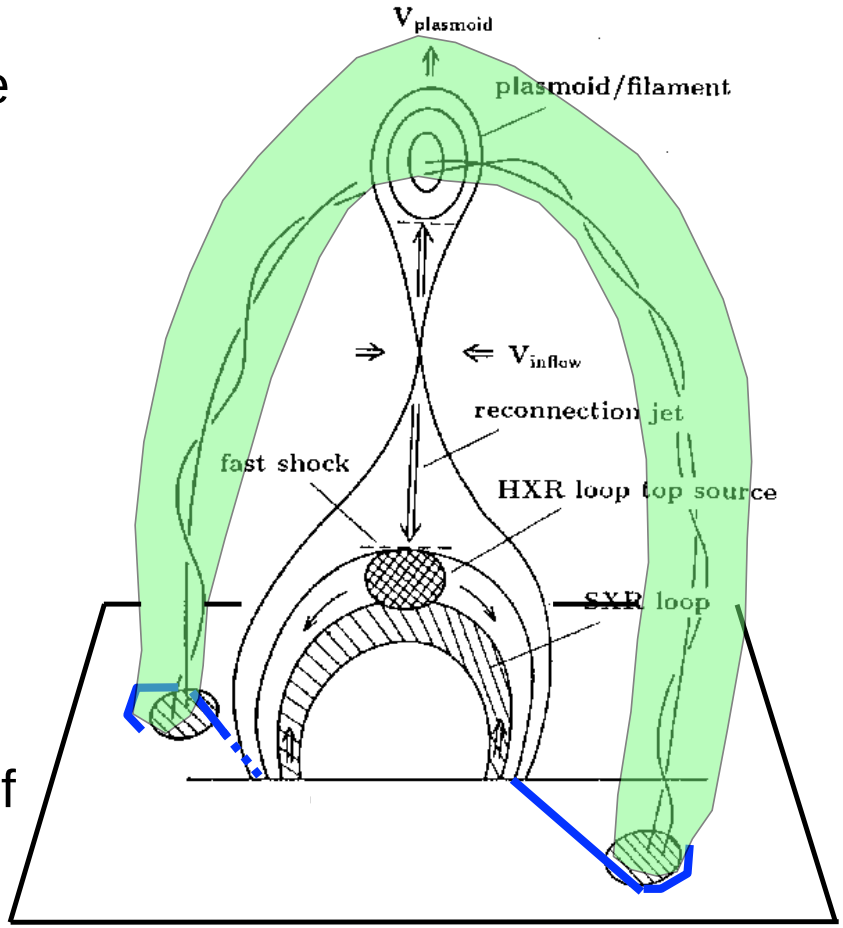

# Evolutionary phases of flare/CME

Zhang et al., 2001, Zhang & Dere, 2006, Vršnak, 2008

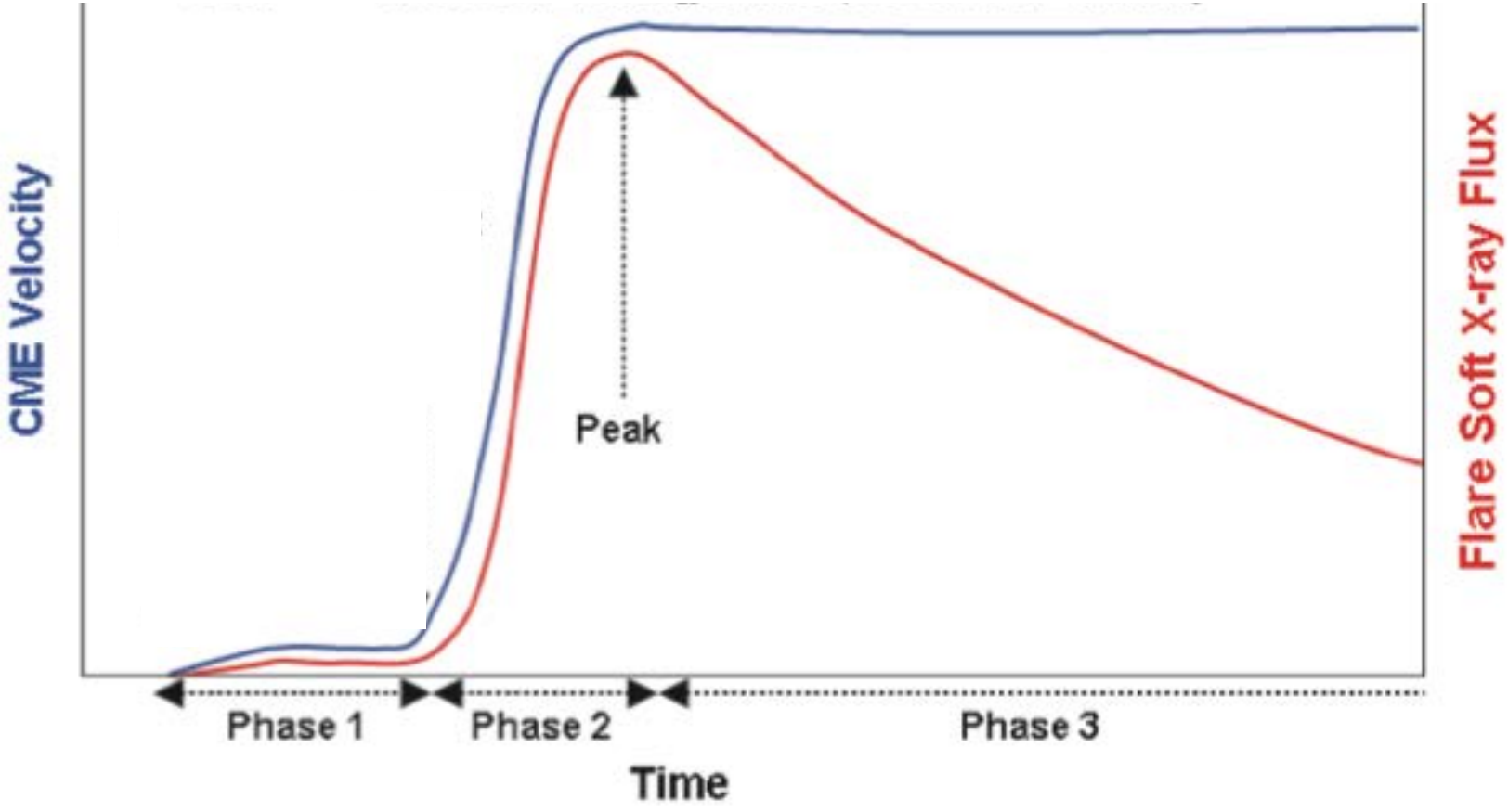

# Standard flare-CME model: CSHKP model

Seminal papers:

- Carmichael 1964
- Sturrock 1966
- Hirayama 1974
- Kopp & Pneuman 1976

# Lower atmospheric signatures: dimmings

Powerful diagnostic of CME early phase

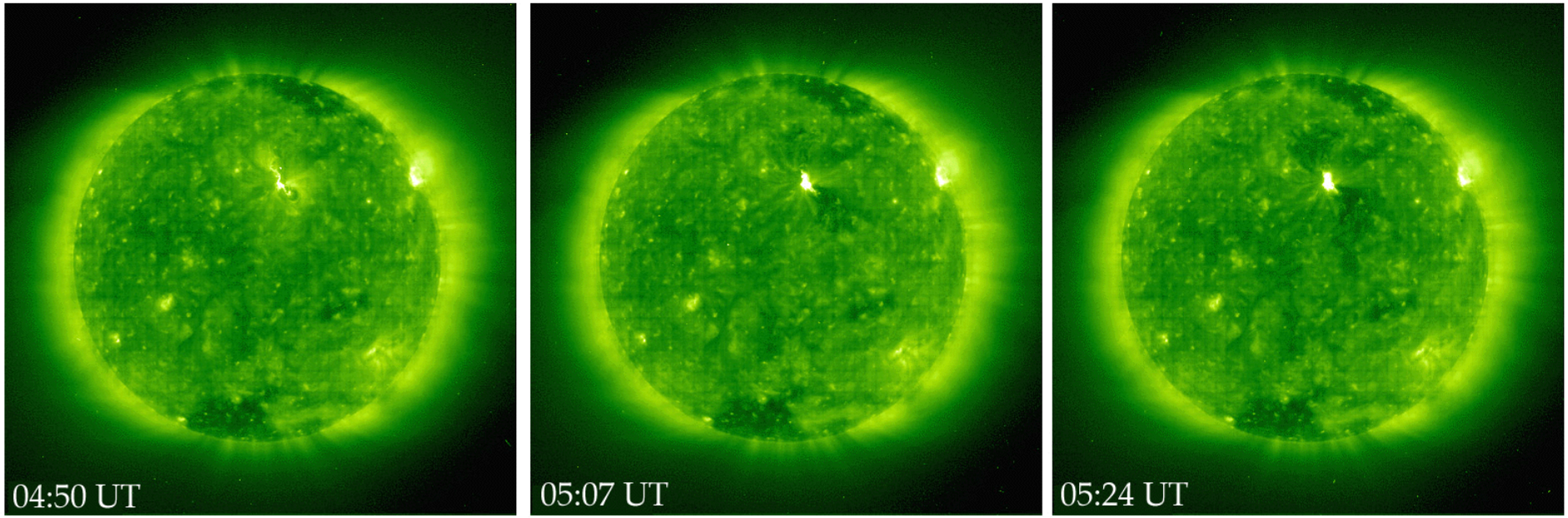


SOHO-Extreme ultraviolet Imaging Telescope (EIT)
observations of postflare loops and coronal mass ejection (CME) cavity
1997 May 12
Fe XII 195 Å (1.5 MK)

# EUV/ soft X-ray dimmings

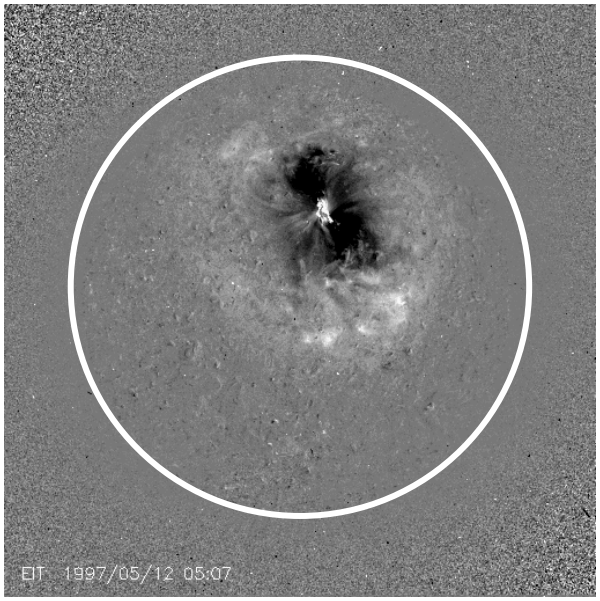


- Rust (1983) called them transient coronal holes
- They are material depletions, because the radiative cooling time for their T and spatial extent exceeds their observed time scales (Hudson et al, 1996)
- Loss of material due to eruption. Indicator of erupting fields?
- Dimmings mark out the footprints of CMEs!

# Lower atmospheric signatures: EUV waves

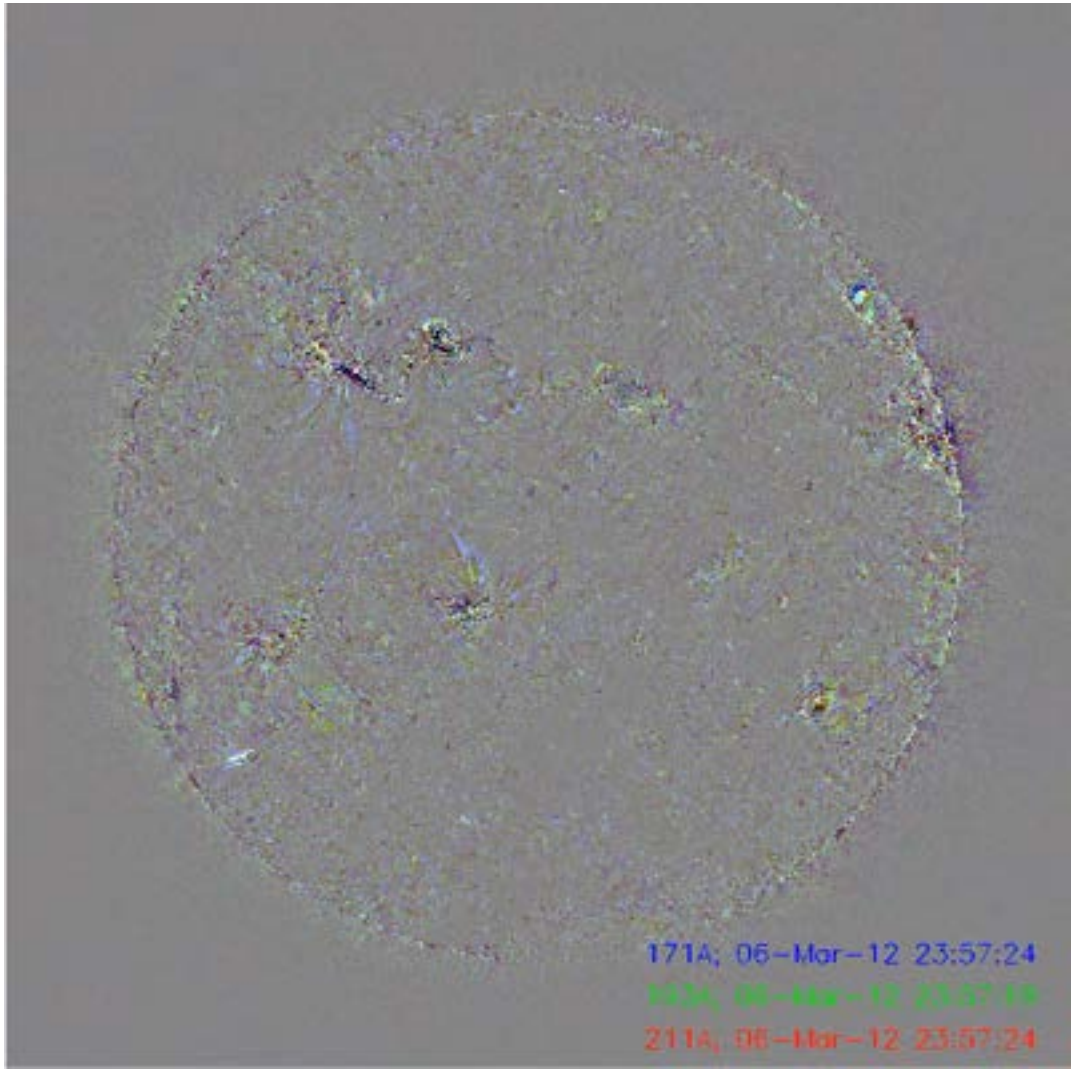


Movie courtesy of David Long

# Energy sources for a CME - estimations!

**Possible energy sources** (for spherical pre-CME volume of radius $10^7$ m, temp 1MK, $n_p$ $10^{15}$ $m^{-3}$, height $10^4$ m, field strength 0.1 T) **include**:

Thermal energy derived from the pre-CME plasma ~ $n_p k_B T$ in vol. V

$n_p k_B TV = 10^{15} \times 1.38 \times 10^{-23} \times 10^6 \times 4 \times 10^{21} \sim 10^{19}$ J

Gravitational potential energy of the pre-CME plasma - $n_p V m_H g_\odot H$

$10^{15} \times 4 \times 10^{21} \times 1.7 \times 10^{-27} \times 274 \times 10^7 \sim 10^{19}$ J

Magnetic energy stored in the coronal magnetic field - $(B^2/2\mu_0)$ V

~ $10^{25}$ J

Total energy in a CME ~ $10^{25}$ J

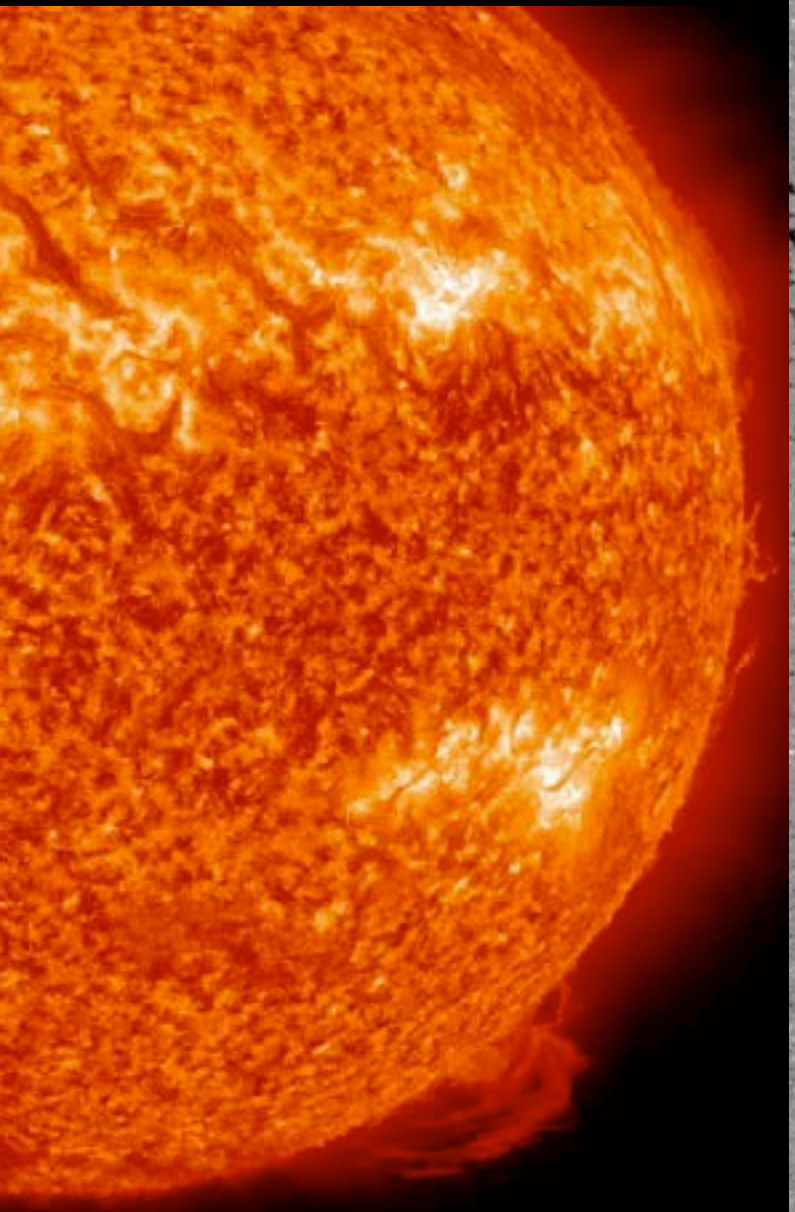

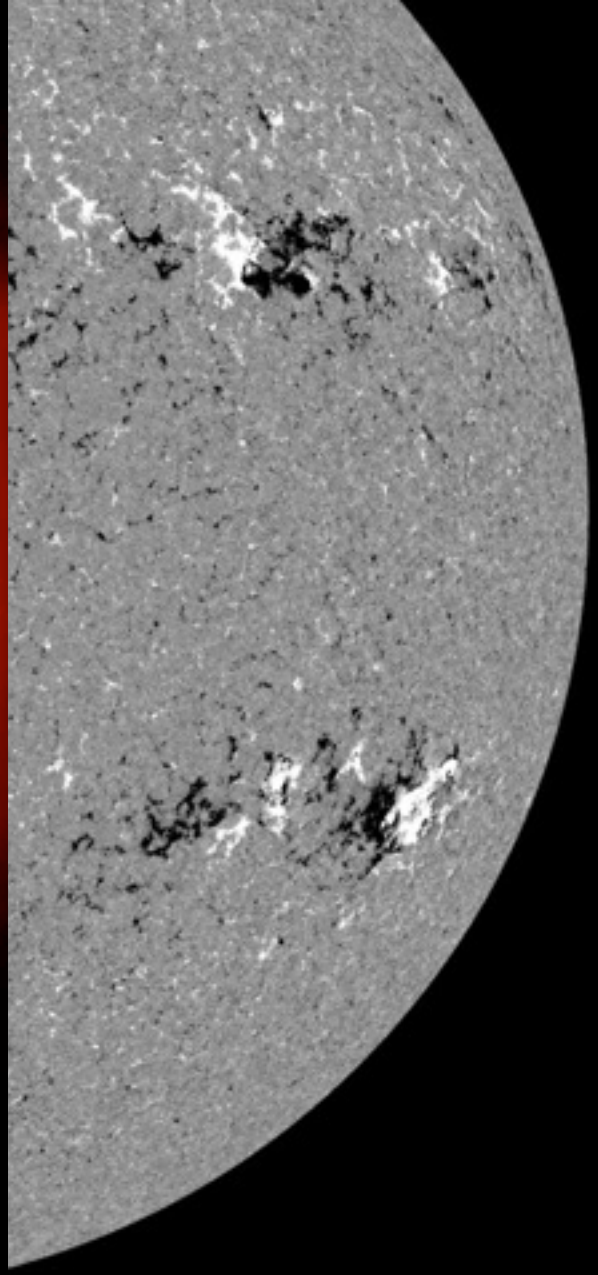

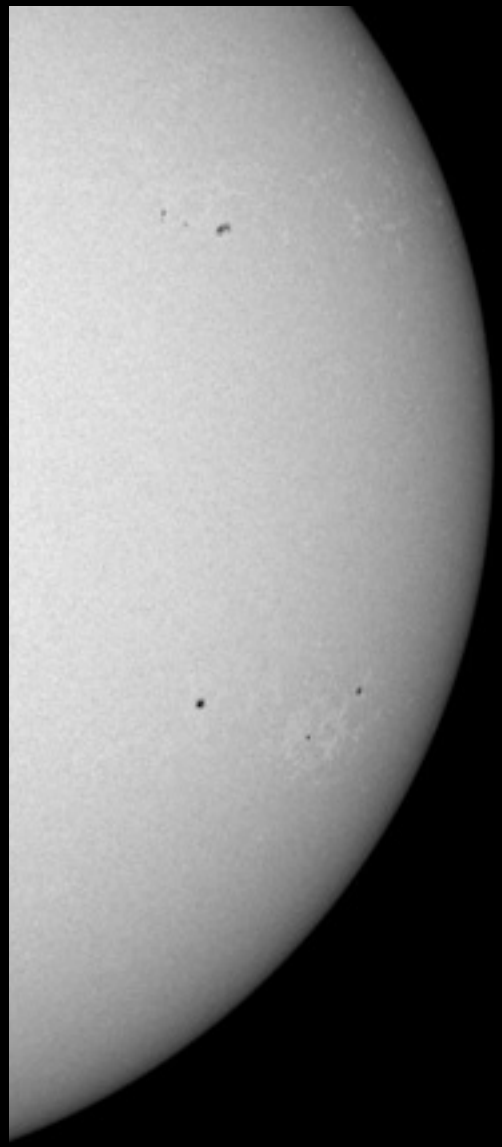

# Spatial scales of CMEs: 10s thousands to 100s thousands km

Mandrini et al., 2005


Su & Ballegooijen, 2013

# CMEs and the solar cycle

Robbrecht et al. 2008

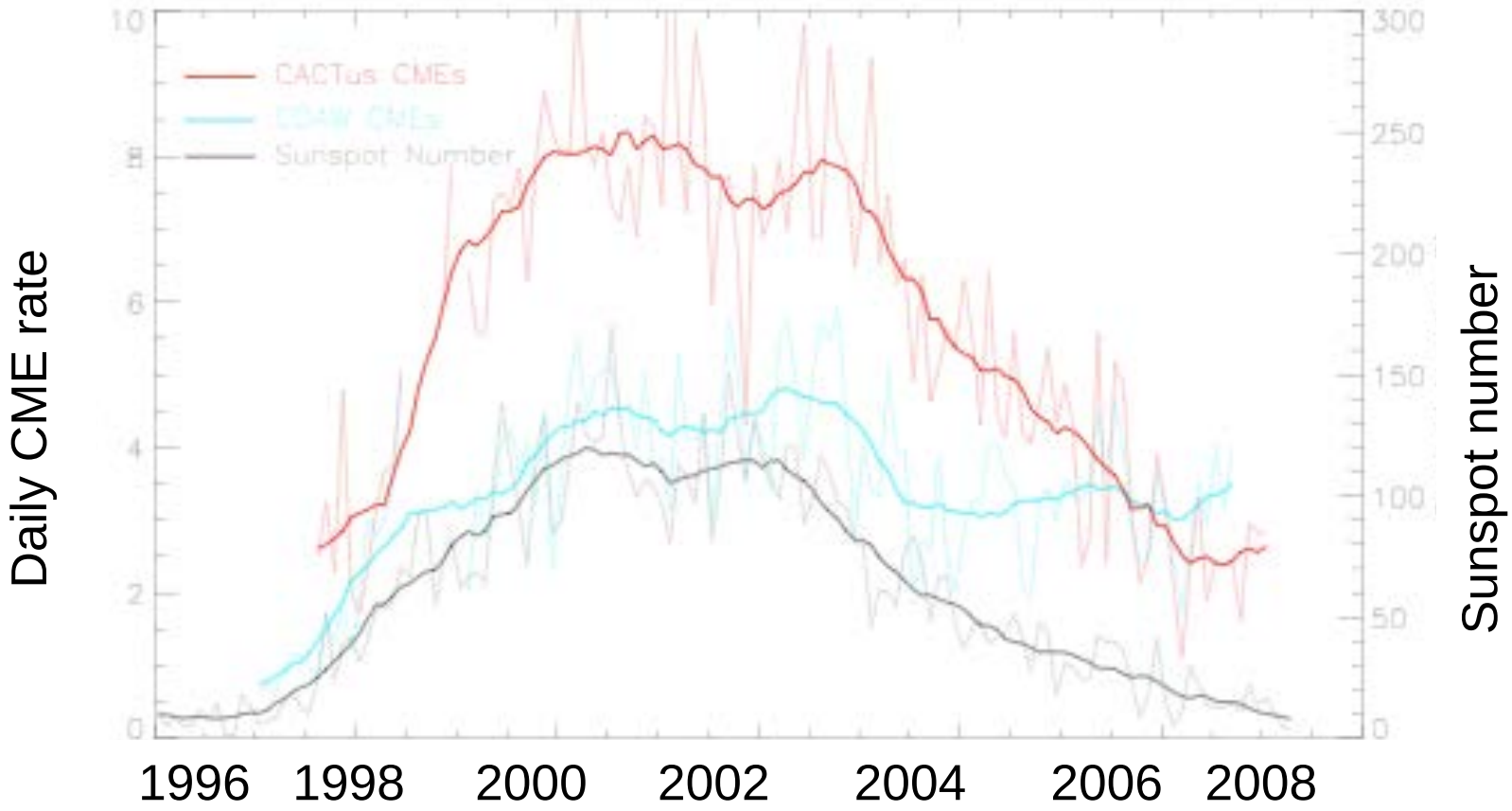

# CMEs and the solar cycle

- There is little change in CME mass and angular size across solar 11-year cycle.
- There is some indication that CME average speeds are higher at maximum than minimum (but not well established).
- Both central latitude and occurrence frequency do show a solar cycle dependence

CME catalogues may be biased by human judgement (blue curve on previous slide), however. Automated catalogues follow the cycle more closely.

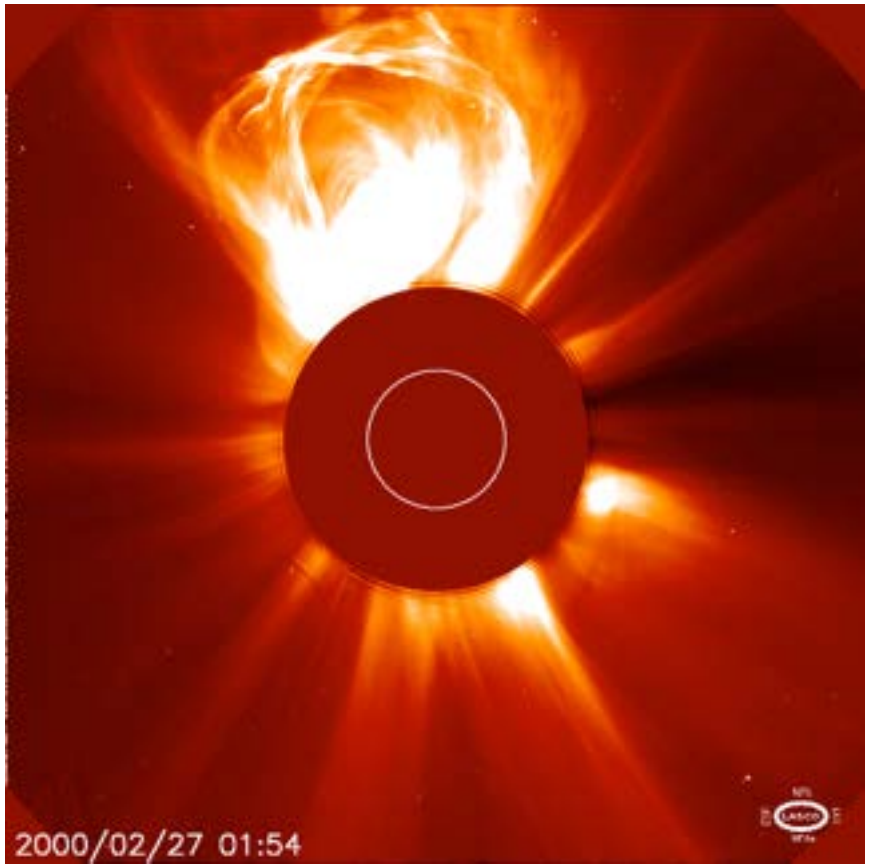


# Coronal mass ejection (CME) models

# CME models

It is generally accepted that the only source of energy large enough to power CME eruptions is the free energy stored in the magnetic field. Kinetic, thermal, gravitational energy densities are not enough for the required energy density of 100 ergs $cm^{-3}$ (Forbes, 2000).

"main phase" of eruption quite well understood: flare ribbons, reconnection etc.

Key questions that CME models must answer:

- How is the energy released/converted into other forms?
- What drives the CME?
- What happens to the overlying field?

From CME models and observations together:

- Do flux ropes exist prior to a CME?

# CME models: resistive models I

**Tether cutting model**

Eruption due to:

- Reconnection is the cause and driver of the eruption
- Runaway magnetic reconnection transforms a sheared arcade into a flux rope, removing overlying stabilising fields (tethers), and increasing the internal magnetic pressure

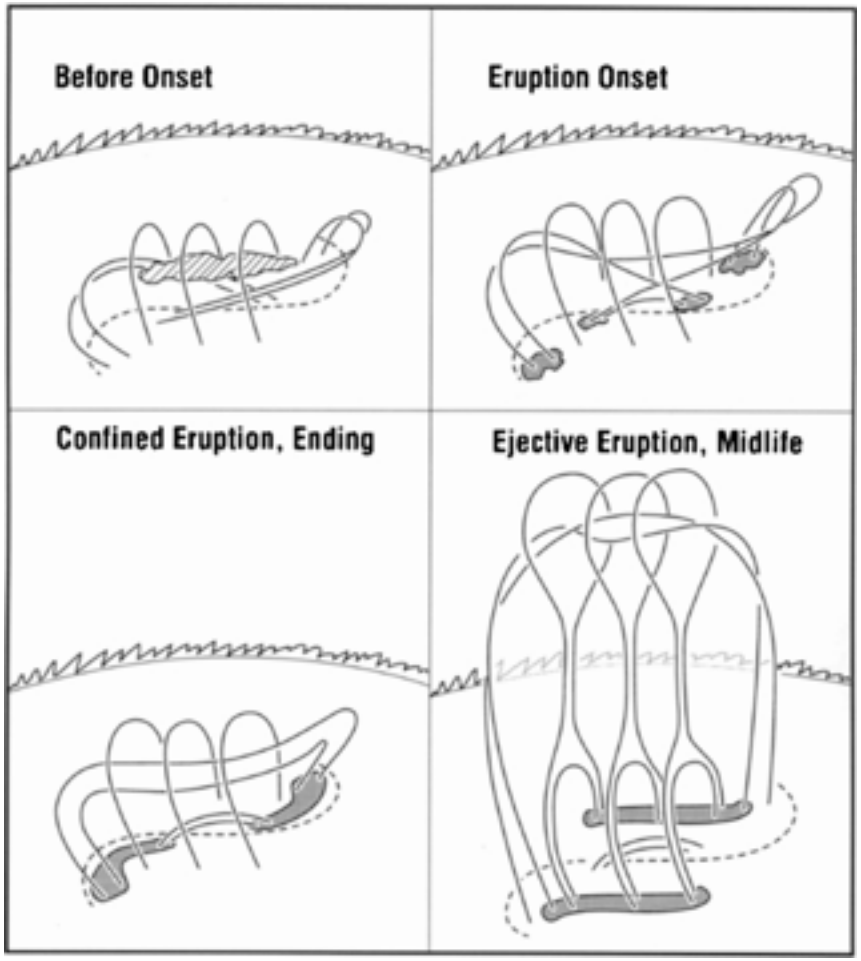


Moore et al., 2001

# CME models: resistive models II

**The breakout model**

Footpoint motions in an arcade shear the central field

The overlying field is removed by reconnection

This allows the underlying sheared field to ‘breakout’ and erupt

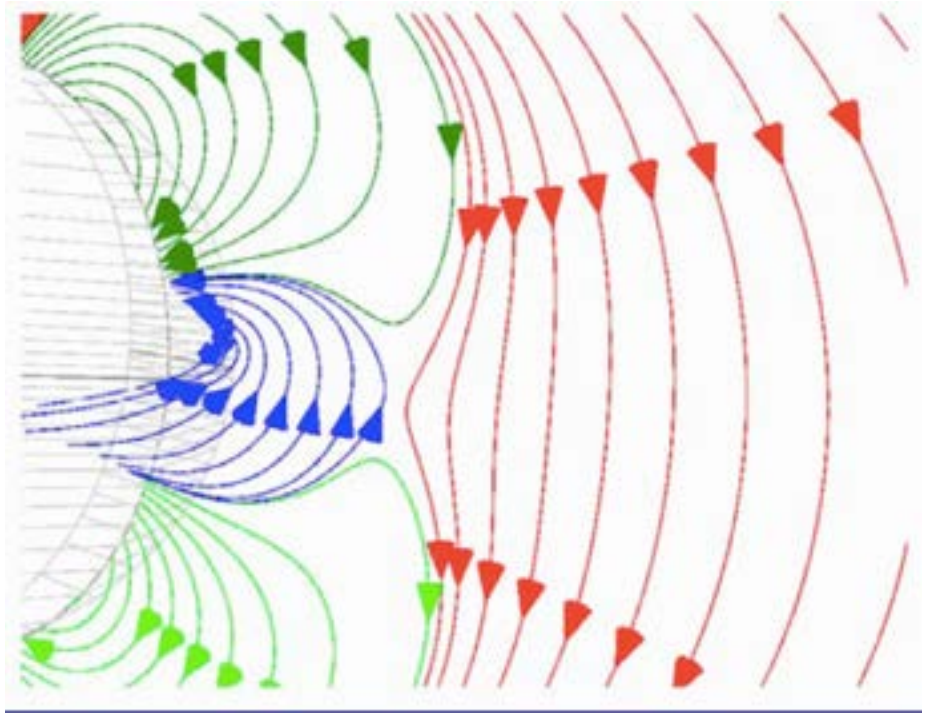

Papers by Antiochos, MacNeince, Lynch

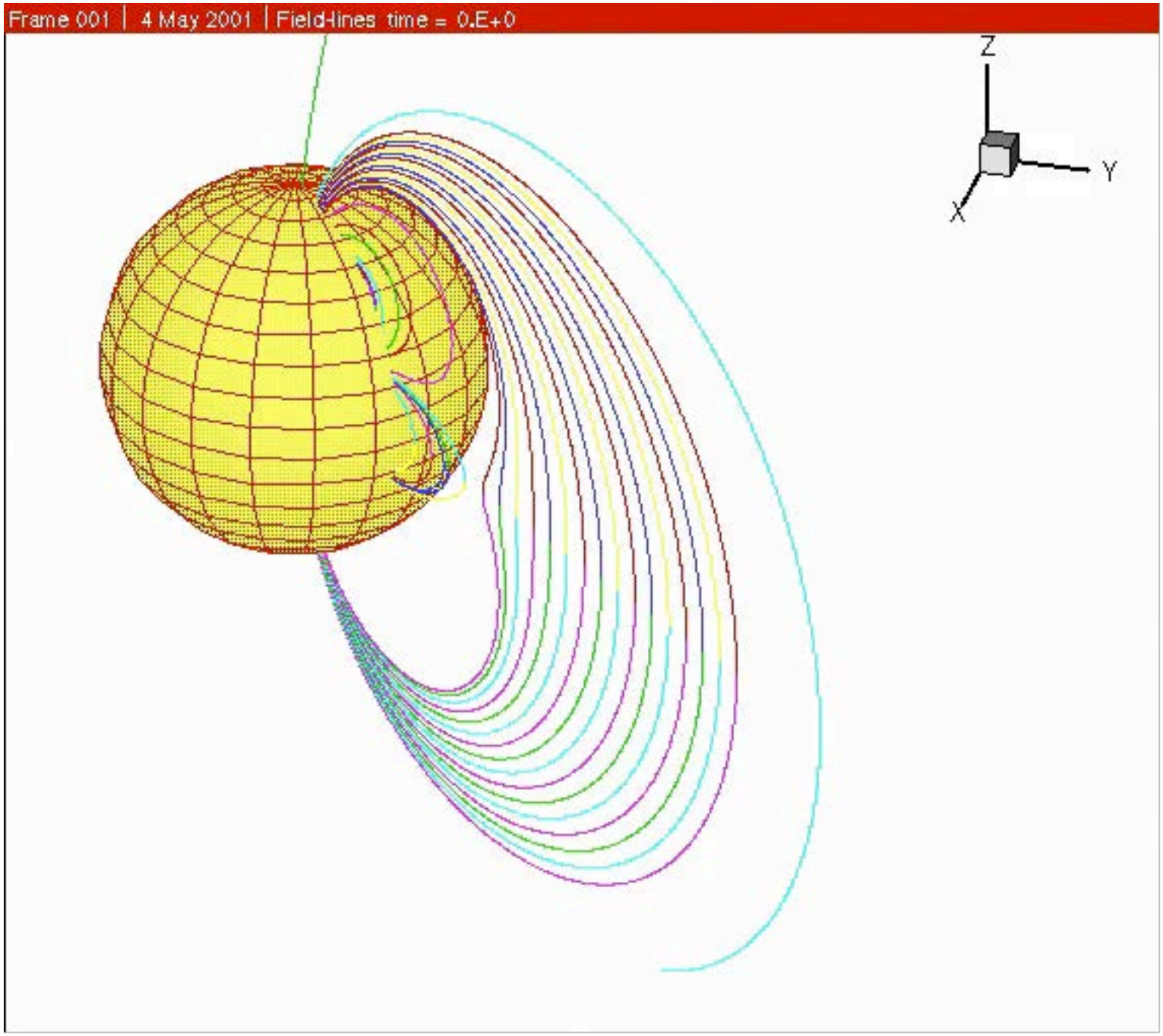
Frame 001 | 4 May 2001 | Field-lines time = 0.E+0
Z
Y
X

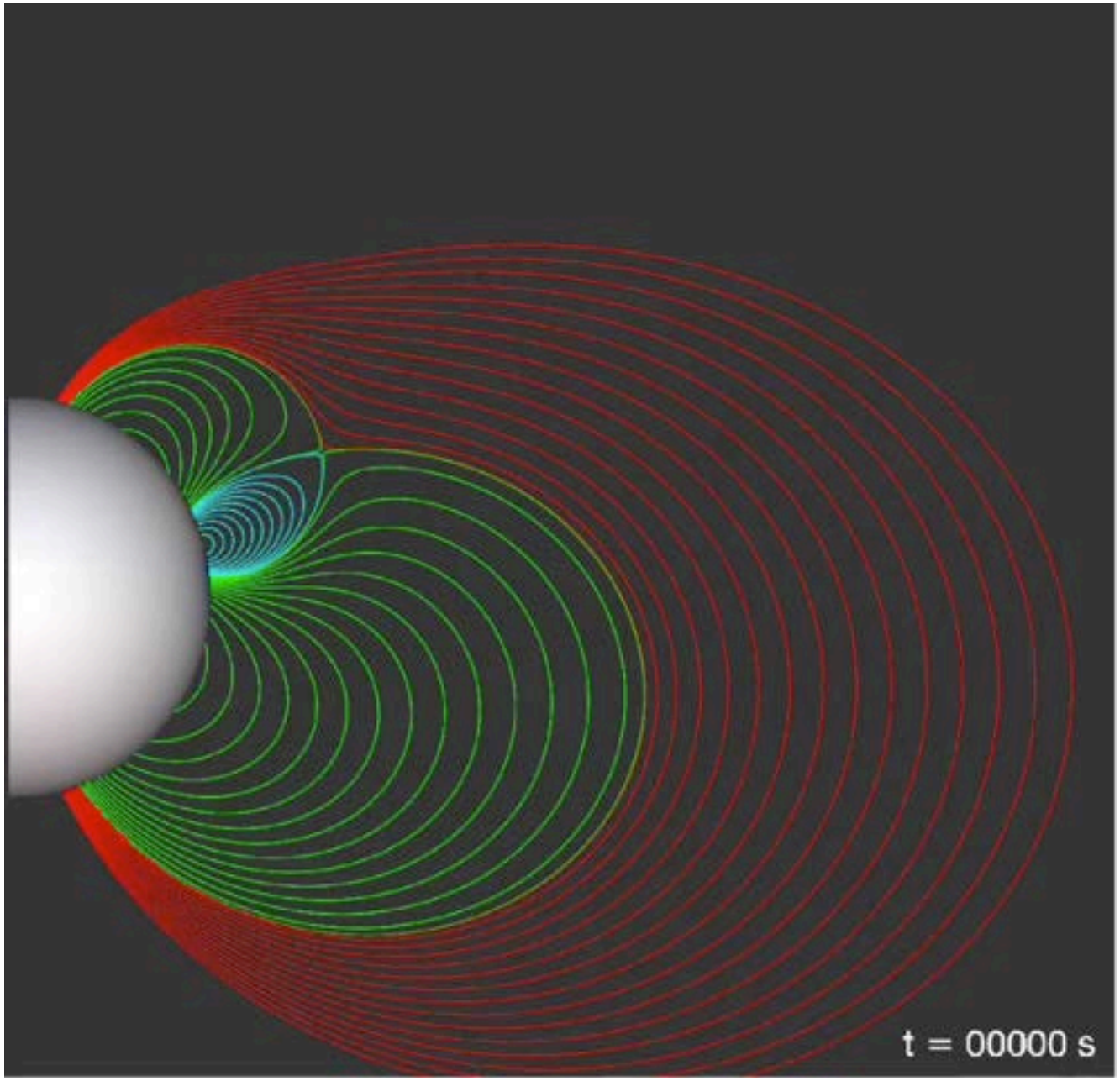


Simulation courtesy of Lynch

# CME models: ideal models I

## Torus instability

- Occurs when the flux rope has a semi-circular shape
- Occurs if the overlying field drops sufficiently with height.
- Driven by hoop force of a flux rope (Lorentz force of a current ring).

(See Kliem and Török, 2006)

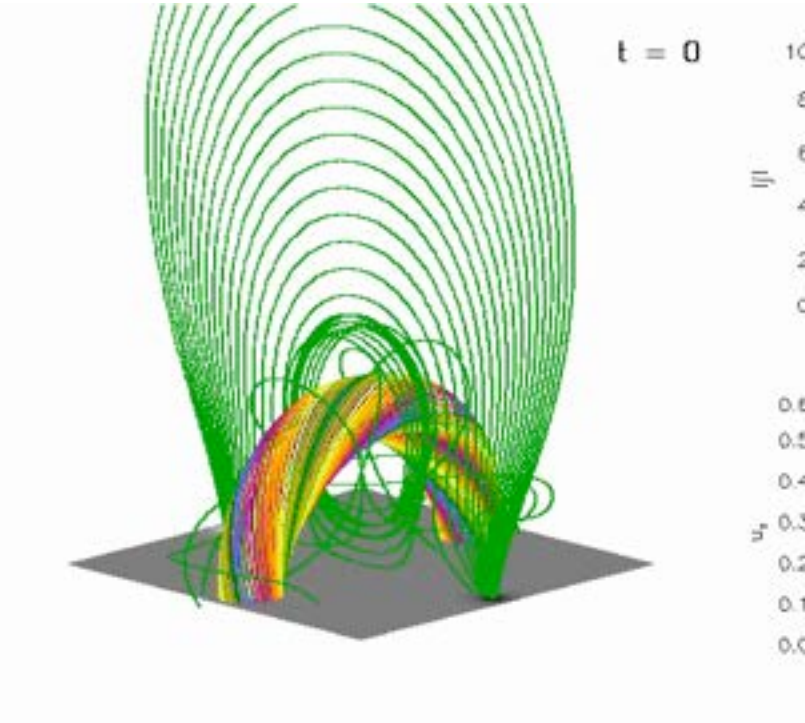


Simulation by B. Kliem

# Flux rope forces

In a curved magnetic flux rope there is an imbalance between axial and azimuthal fields: The loop's curvature packs the azimuthal field lines together more densely at the inner edge, so the azimuthal field (associated with the twist in the loop) will be more intense at the inner edge of the loop apex than at the outer.

- The resulting gradient of the magnetic pressure $p_m=B^2/2\mu_0$ will tend to expand the loop outward against the tensions of the axial field lines.

- In equilibrium, the difference of these two forces must be balanced by downward acceleration of gravity on the plasma contained in the rope and tension of the overlying field.

- Instability sets in when equilibrium is lost due to e.g. changes in the tension of the restraining overlying field.

$(B_{\parallel}\nabla)B_{\parallel}$

$$\nabla\frac{B^2}{2\mu_0}$$

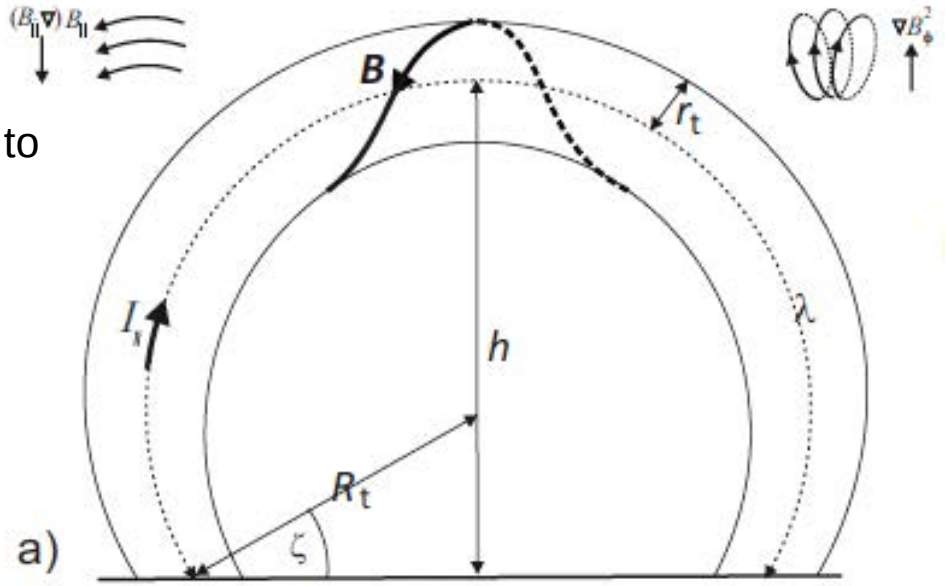


(See Shafranov, 1966 and Chen, 1989)

Image courtesy of B. Vrsnak

# CME models: ideal models II

## Kink instability

- Occurs when twist in flux rope exceeds a critical value of ~5 π (2.5 full turns) (Priest & Hood, 1979).
- Driven by conversion of twist into writhe.
- Effect: makes a flux rope “arch up”, may be followed by the Torus instability

Simulation by Tibor Török

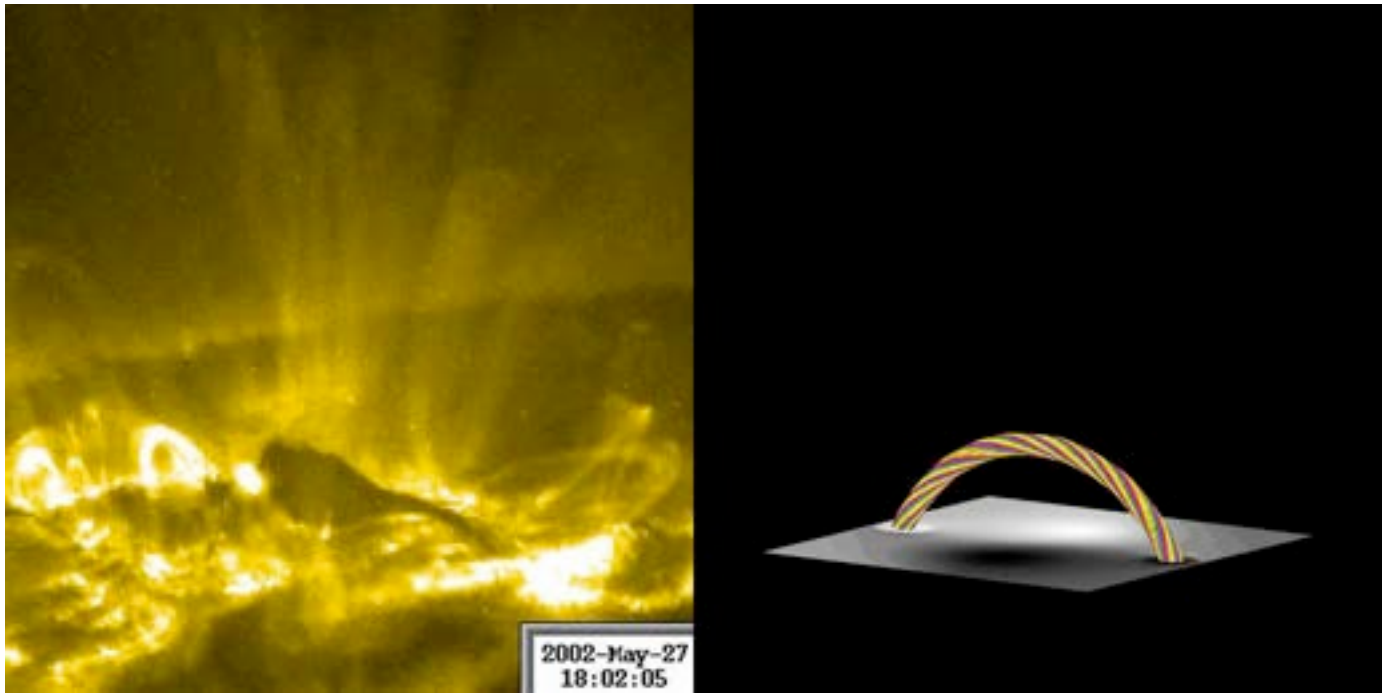

# CME models: ideal models and flux ropes

**Flux rope present before the eruption**

- Loss of equilibrium (Forbes & Isenberg 1991) & force imbalance (van Ballegooijen & Mackay 2007)
- Ideal MHD instability (Török & Kliem 2005; Kliem & Török 2006)

# Ideal models require a pre-eruption flux rope

van Ballegooijen & Martens, 1989

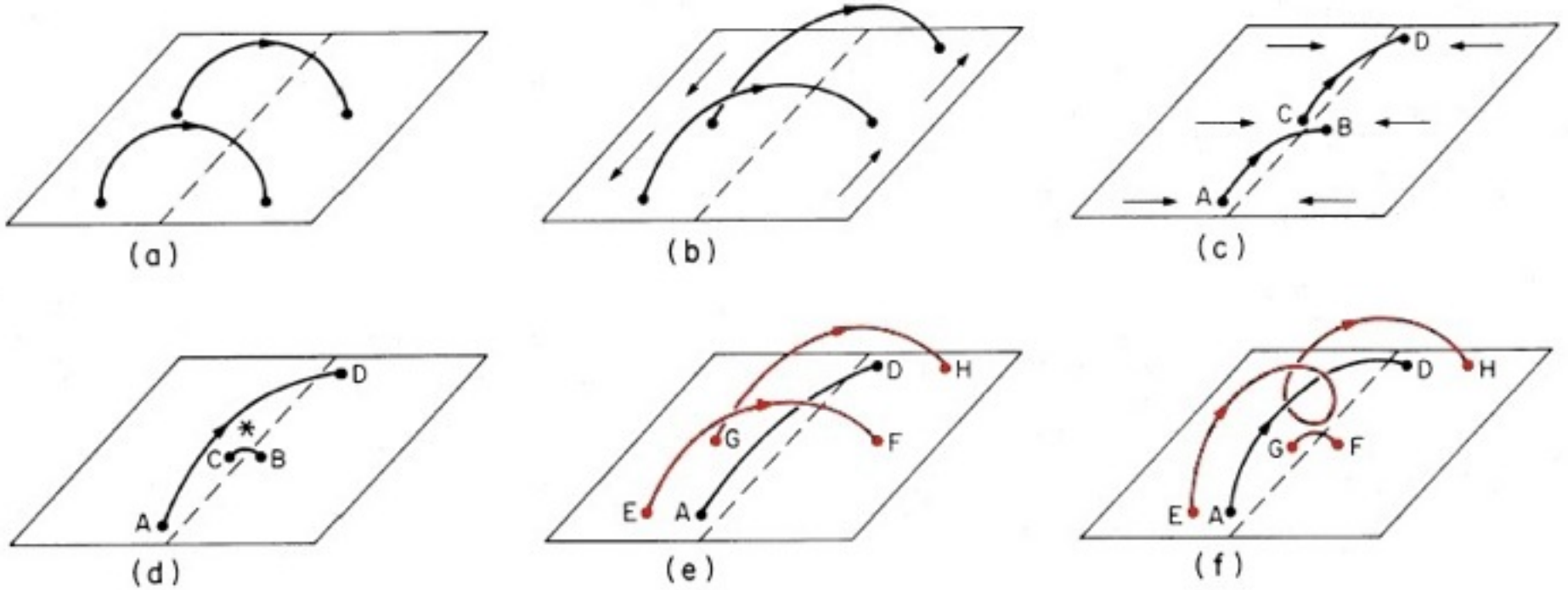

# Example active region evolution

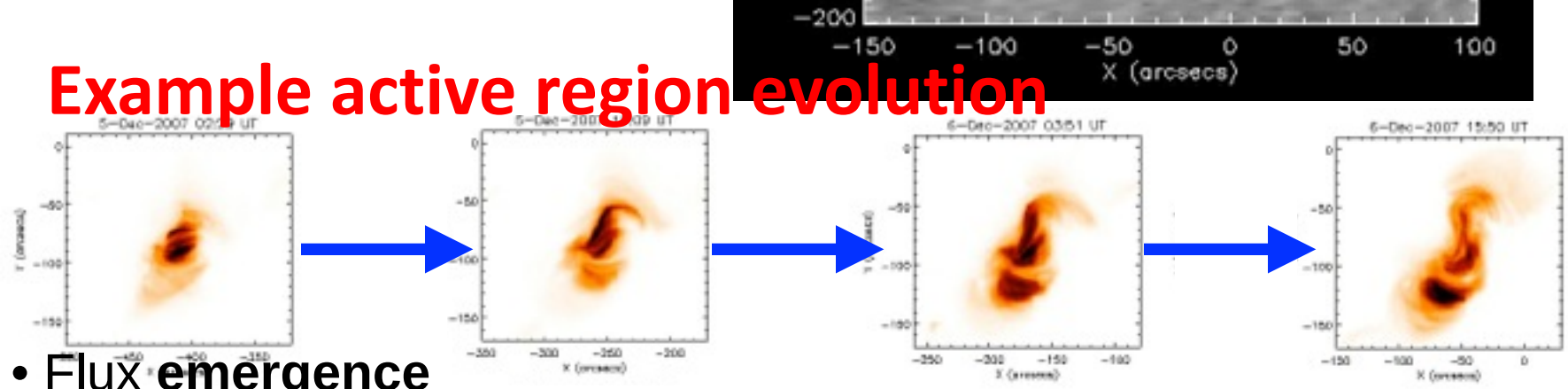


- Flux **emergence**
- Flux **fragmentation** and **dispersal**
- **Elongation** along the Y direction
- Flux **cancellation**

# Flux rope formation

van Ballegooijen & Martens, 1989

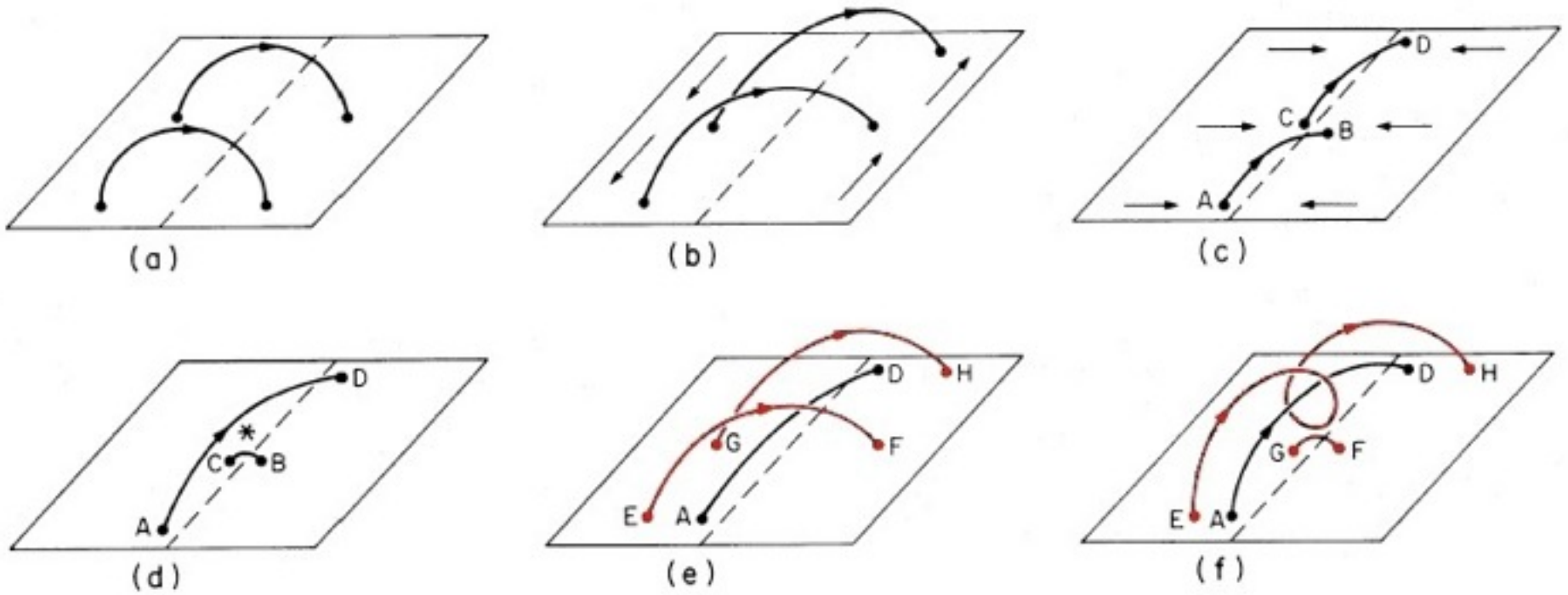


Green, Kliem & Wallace, 2011; Savcheva et al., 2012; Green & Kliem, 2014

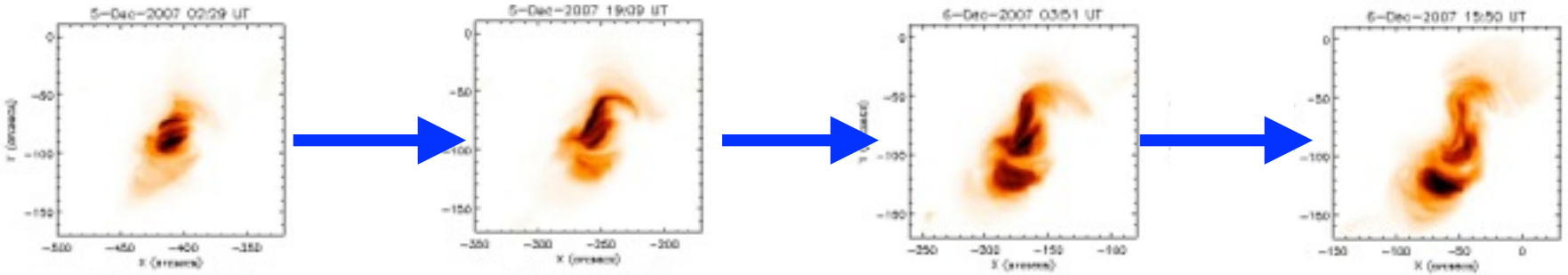

# CME models: essential features

- Pre-eruptive configuration: stressed core-field + stabilizing overlying field.
- All models produce a vertical current sheet under the erupting structure → flare.
- All models involve a flux rope at some point.

(growing evidence for pre-eruption flux ropes)

**TRIGGER**: any mechanism that slowly drives or dynamically perturbs the pre-eruptive configuration and brings it to the point of eruption

**DRIVER**: any mechanism which can account for rapid (exponential) acceleration and huge expansion of the core field / flux rope

Green et al., submitted, 2017

| MECHANISM | REFERENCES |
|---|---|
| TRIGGER: Mass (un-)loading | Low (1996); Fong et al (2002); Zhang and Low (2004); Seaton et al (2011) |
| Sunspot rotation | Amari et al (1996b); Tokman and Bellan (2002); Török and Kliem (2003); Aulanier et al (2005); Rachmeler et al (2009) |
| Twisting overlying field | Török et al (2013) |
| Shearing of arcade | Mikic et al (1988); Biskamp and Welter (1989); Mikic and Linker (1994); Choe and Lee (1996a,b); Amari et al (1996a); Jacobs et al (2006, 2009); Roussev et al (2007); Shiota et al (2008); Downs et al (2011) |
| Reversed shear | Kusano et al (2004) |
| Self-induced shear flows | Manchester (2003, 2007); Manchester et al (2004a) |
| Magnetic breakout | Antiochos et al (1999); MacNeice et al (2004); Lynch et al (2004, 2008); van der Holst et al (2007, 2009); Masson et al (2013) |
| Tether cutting | Moore and Roumeliotis (1992); Moore et al (2001); Aulanier et al (2010) |
| Converging flows / Flux cancellation | Inhester et al (1992); Amari et al (2003a); Roussev et al (2004); Zuccarello et al (2012); Mikić et al (2013) |
| Flux decrease / dispersion | Lin et al (1998); Linker et al (2001, 2003); Amari et al (2000, 2003b); Titov et al (2008); Reeves et al (2010) |
| FE close/below flux rope | Chen and Shibata (2000); Lin et al (2001); Shiota et al (2005); Dubey et al (2006) |
| FE into potential arcade | Zuccarello et al (2008); Jacobs and Poedts (2012); Roussev et al (2012) |
| FE into sheared arcade | Notoya et al (2007); Kusano et al (2012) |
| Helical kink instability | Sakurai (1976); Hood and Priest (1979); Gerrard et al (2001); Fan and Gibson (2003); Török et al (2004); Török and Kliem (2005) |
| Flux transfer/feeding | Zhang et al (2014) |
| Tilt instability | Keppens et al (2014) |
| Double-arc instability | Ishiguro and Kusano (2017) |

Green et al., submitted, 2017

| | |
|---|---|
| DRIVER:<br>Torus instability<br>/ Flux-rope catastrophe<br>/ Loss of equilibrium | van Tend and Kuperus (1978); Priest and Forbes (1990); Forbes and Isenberg (1991); Lin et al (1998); Kliem and Török (2006); Török and Kliem (2007); Fan and Gibson (2007); Olmedo and Zhang (2010); Démoulin and Aulanier (2010); Kliem et al (2014) |
| Flare–reconnection | Lin and Forbes (2000); Vršnak (2008); Temmer et al (2010); Karpen et al (2012) |
| Review articles: | Forbes (2000); Chen (2001); Klimchuk (2001); Low (2001); Priest and Forbes (2002); Lin et al (2003); Linker et al (2003); Zhang and Low (2005); Forbes et al (2006); Moore and Sterling (2006); Mikić and Lee (2006); Roussev (2008); Vršnak (2008); Amari and Aly (2009); Linton and Moldwin (2009); Schrijver (2009); Aulanier et al (2010); Chen (2011); Jacobs and Poedts (2011); Kleimann (2012); Schmieder et al (2013); Aulanier (2014); Schmieder et al (2015); Inoue (2016) |

In observed events probably elements from most current models play some role!

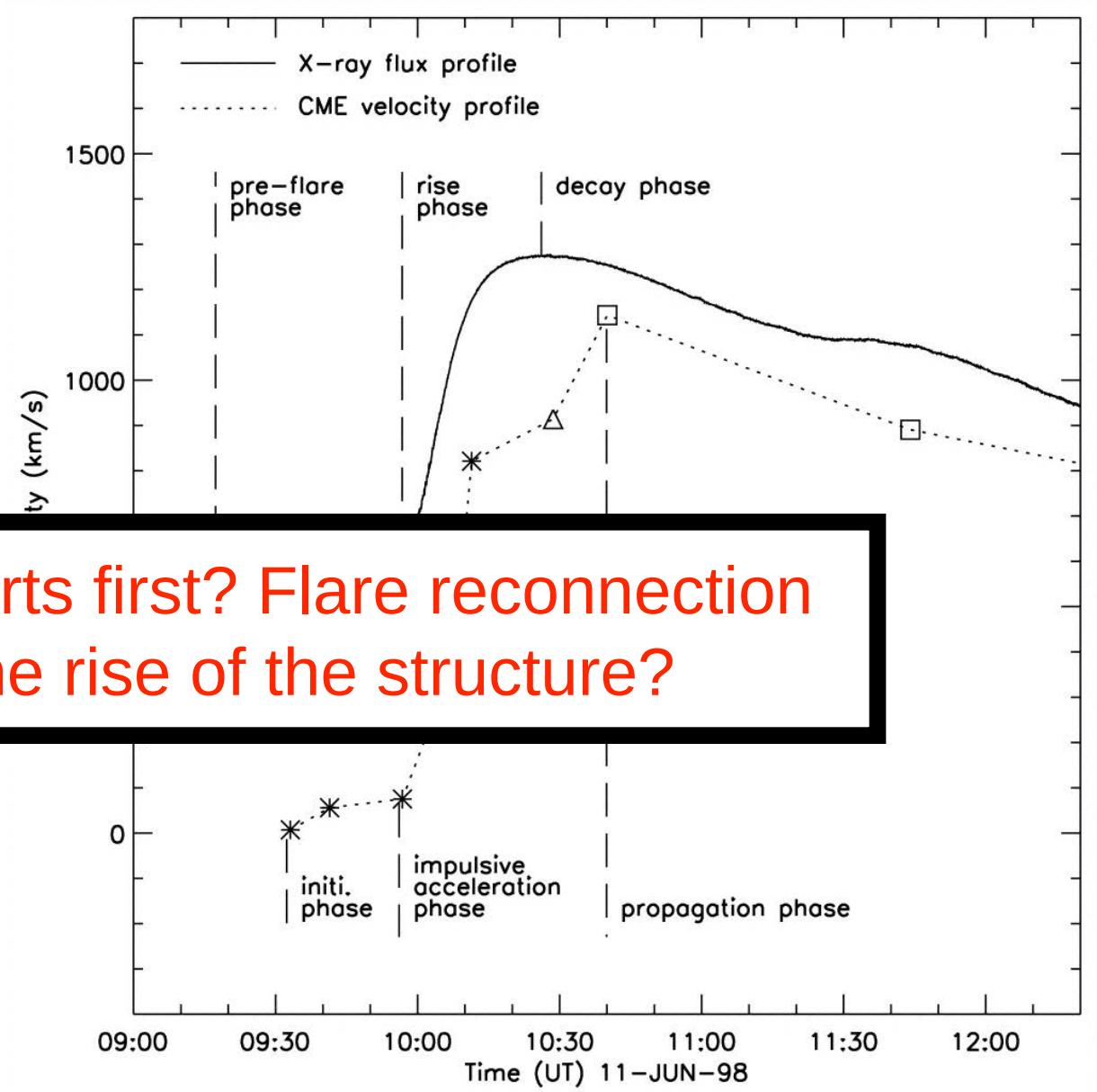


What starts first? Flare reconnection or the rise of the structure?

Zhang et al. 2001

# Concluding remarks about CMEs

Does the pre-eruption structure necessarily have a flux-rope topology?

Does an eruption begin as an ideal process (i.e. no reconnection in the early stages)?

Does reconnection occur above the main eruption structure (break-out) or under it (tether cutting)?

Is there a particular photospheric flow pattern leading up to eruption?

# The solar wind

# The solar wind: history

- 27-day recurrence period of strong aurorae lasting for several solar rotations.
- ⇒ corpuscular emissions travel from the Sun to Earth.
- Biermann (1951) argued that solar radiation pressure (suggested by Galileo) was not enough to explain acceleration of plasma structures within comet tails and twin-tail structures. The deviation of the comet tails from the Sun-comet vector could best be explained by a “solar corpuscular radiation”, i.e. plasma pressure of continuous radial outflow of charged particles from the Sun, with a varying speed. He suggested speeds of v ~ 500-1000 km $s^{-1}$.
- However, nobody could give a good reason why this “particle radiation” should exist…

# The solar wind: summary

Above the solar surface is a tenuous gas at $T > 10^6$ K:

- high-thermal conductivity ensures high temperature out to a large height
- high pressure relative to interstellar medium
- corona extends into interplanetary space.

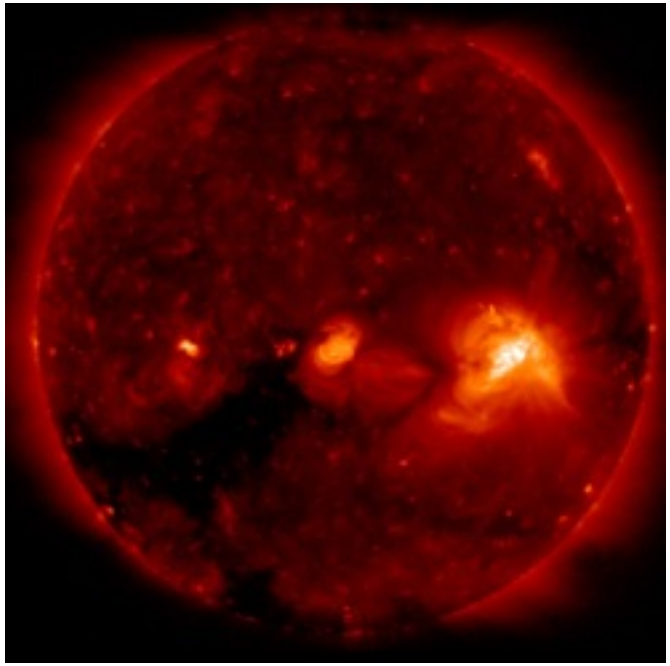

Hinode/XRT image of the X-ray emitting corona

There is, at all times and all latitudes relative to the ecliptic, an outflow of particles traveling at several hundreds of km $s^{-1}$.

The existence of the solar wind was predicted several years before it was actually observed by in situ instrumentation, primarily through the work of Chapman and Parker in 1957-58.

# Thermal conductivity of the corona

- Chapman (1957): the corona has high thermal conductivity and hence will not be confined.
- The high thermal conductivity in the corona implies very efficient outward (and inward) heat transport from the inner corona.
- Taking outward heat conduction as the only heat source to a steady corona (no heating by radiation), the **coronal energy balance obeys the relation**:

$$F_c = 4\pi r^2 \kappa \frac{dT}{dr}$$

where $F_c$ is the constant conductive flux, r is heliocentric distance, and κ is the thermal conductivity:

$$\kappa = \kappa_0 T^{5/2}$$

Integrating the equation we get the temperature profile of the corona:

$$T(r) = T_0 (r / R_0)^{-2/7}$$

where $T_0 = T(r_0)$ and T is assumed to vanish at r = ∞

- High thermal conductivity → slow decrease of T : at 1 AU ~2.2 x $10^5$ K.

# Thermal conductivity of the corona

- For hydrostatic equilibrium $$\frac{dP}{dr} = \frac{GM_\odot \rho}{r^2}$$

where G is gravitational constant and $M_\odot$ is the Sun's mass.

If the particle density is n and we have a pure H atmosphere, then $\rho = n(m_e + m_p) \sim n m_p$ assuming $T_e = T_p$ and $P = 2nkT$ holds, then the solution is:

$$P(r) = P_0 \exp\left\{-\frac{7}{5}\frac{GM_\odot m}{2kT_0 r_0}\left[1-\left(\frac{r}{r_0}\right)^{-5/7}\right]\right\}$$

**Pressure decreases steadily outward, but never reaches zero.**

Parker (1958): the corresponding relatively high pressure at infinity presents a difficulty in matching values with the lower pressure expected in the ISM (interstellar medium):

- for ionized H: $P \sim 0.6\ 10^{-6}$ Pa
- for neutral H: $P \sim 1.e\ 10^{-10}$ Pa

The interstellar gas pressure is $P \sim 1.4\ 10^{-14}$ Pa - much smaller than either value.

# The dawn of the solar wind

In planetary atmospheres an equilibrium situation evolves between the gravity of the planet and the escape of high-velocity particles, e.g. the Earth's atmosphere gets gradually cooler with increasing distance, with a cool top in equilibrium with the surrounding space.

For the Sun, however, Parker suggested that the conduction of heat interfered with such an equilibrium, and as a result the topmost layers of the corona flowed away from the Sun at a velocity like that of Biermann's "corpuscular radiation."

Parker concluded that:

- *"…probably it is not possible for the solar corona, or indeed, perhaps the atmosphere of any star, to be in complete hydrostatic equilibrium out to large distances. We expect always to find some continued outward hydrodynamic expansion of gas."*

In 1958 he put forward a hydrodynamic model of a continuously expanding corona, or solar wind. He predicted an outward velocity of ~ 1000 km $s^{-1}$.

# Parker's solar wind

Parker proposed a steady flow of plasma from the Sun, rather than a static model

He started with the conservation equations (mass, momentum and energy) and derived an equation of motion, using boundary conditions to eliminate unphysical solutions.

Steady flow means time derivatives are zero. Parker's assumptions:
- solar wind is an ideal gas
- it flows radially away from the Sun
- electromagnetic forces in the wind are negligible
- changes are slow compared to the wind generation timescale
- the wind is isothermal
- mass is conserved in a flow across a spherical surface
- the system is spherically symmetric, i.e. all variables are functions of heliocentric distance, r, only.

**He derived an equation of motion, that reveals the existence of the solar wind:**

$$\frac{1}{u}\frac{du}{dr}\left(u^2 - \frac{2kT}{m}\right) = \frac{4kT}{mr} - \frac{GM_\Theta}{r^2}$$

$$\frac{1}{u}\frac{du}{dr}\left(u^2 - \frac{2kT}{m}\right) = \frac{4kT}{mr} - \frac{GM_\Theta}{r^2}$$

For temperature, T, at the base of the corona the 2nd term on the RHS of equation is larger than the 1st term.

⇒ despite its high T, the corona is gravitationally bound.

Therefore, near the base of the corona the RHS of eqn is < 0.

However, $GM_\Theta/r^2$ falls off more rapidly with r than 4kT/mr so the RHS of eqn increases with increasing r and passes through zero at the critical radius, $r_c$:

$$r_c = \frac{GM_\Theta m}{4kT}$$

and becomes >0 at larger r. This behaviour of the RHS of the eqn influences the nature of its solutions.

# Parker's solar wind: solutions

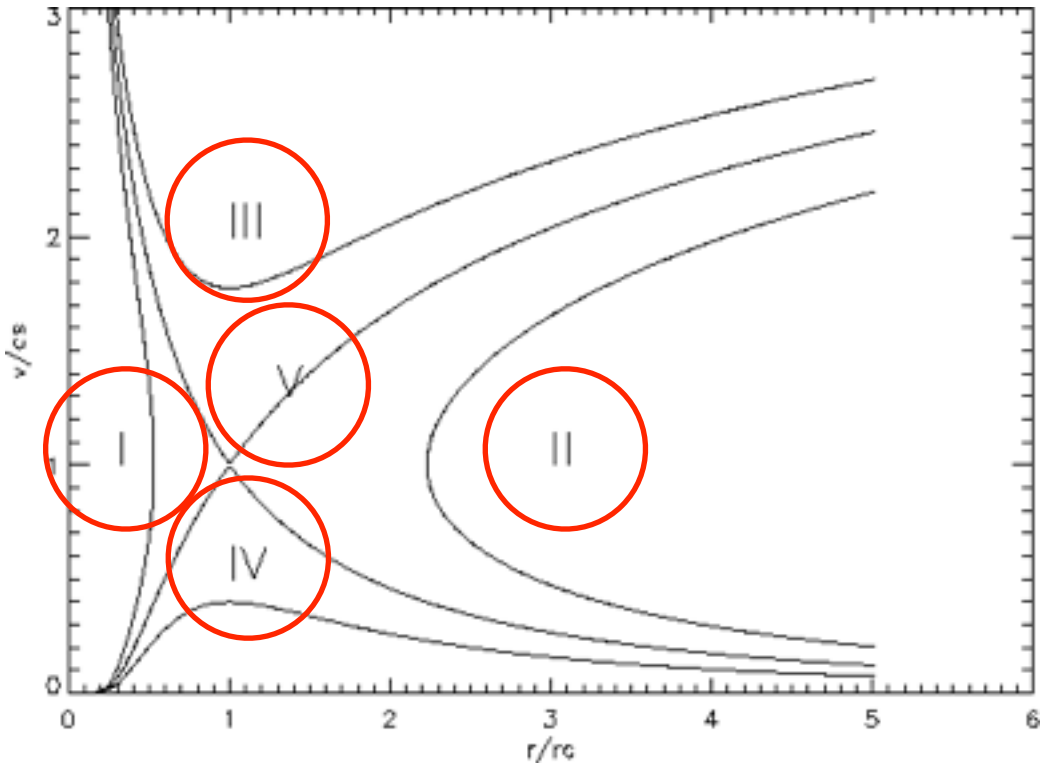


I and II are double valued and confined to small and large radii - EXCLUDED

Solutions of class III do not satisfy the observation that general plasma velocities near the Sun are sub-sonic - EXCLUDED

Solutions of class IV are sub-sonic everywhere and they predict speeds at ~ 1 km $s^{-1}$ at 1 AU. These are the so-called solar breeze solutions favoured by Chamberlain in the late 50s.

Class V starts subsonically near the Sun and reaches supersonic speeds at a critical point (at 10-20 $R_\odot$ ), where du/dr is undefined at $u=u_c$, $r=r_c$. At this point the coefficient of du/dr and the RHS of the motion equation vanish simultaneously.

Acceptance of the solar wind solution that passes through the critical point didn't come until Mariner 2 in situ measurements in 1962 showed the high plasma velocities of the order predicted by Parker (and a 27-day variation of this speed, indicating a connection with solar rotation).

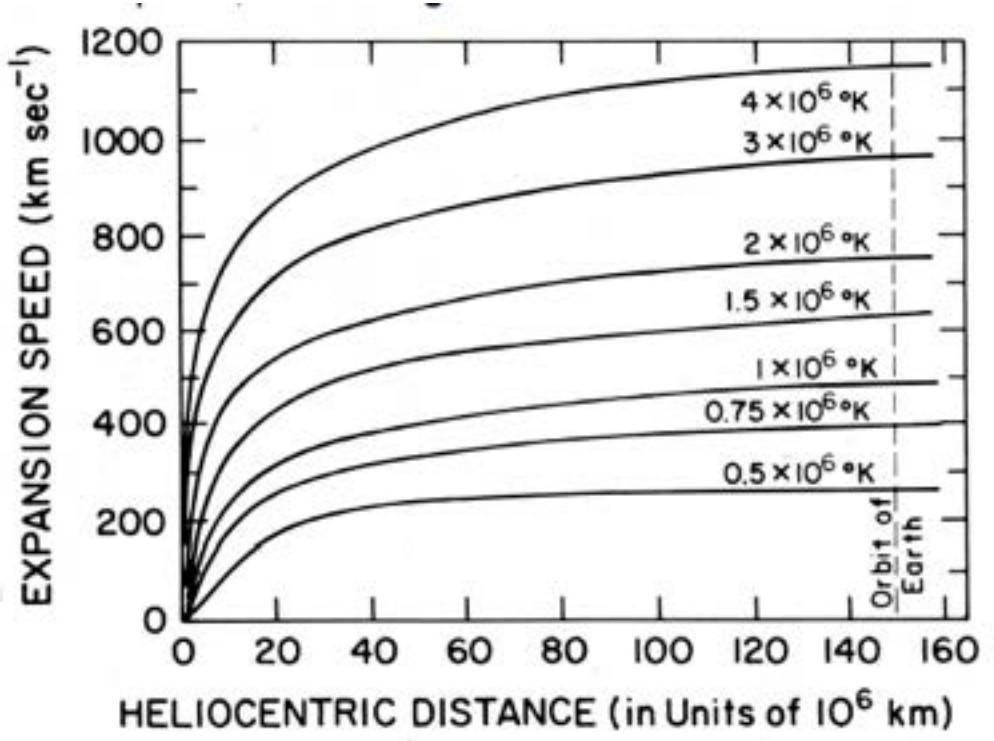


Radial expansion speed of the solar wind derived from the isothermal coronal-expansion models with coronal temperatures ranging from 0.5 x $10^6$ K to 4 x $10^6$ K.

The observed Parker-type speed is 700-800 km/s. The coronal base T in the plot is 2 x $10^6$ K – too high compared to observed values → some kind of additional acceleration in the low corona is needed to reach the observed wind speed.

McComas et al., 2003

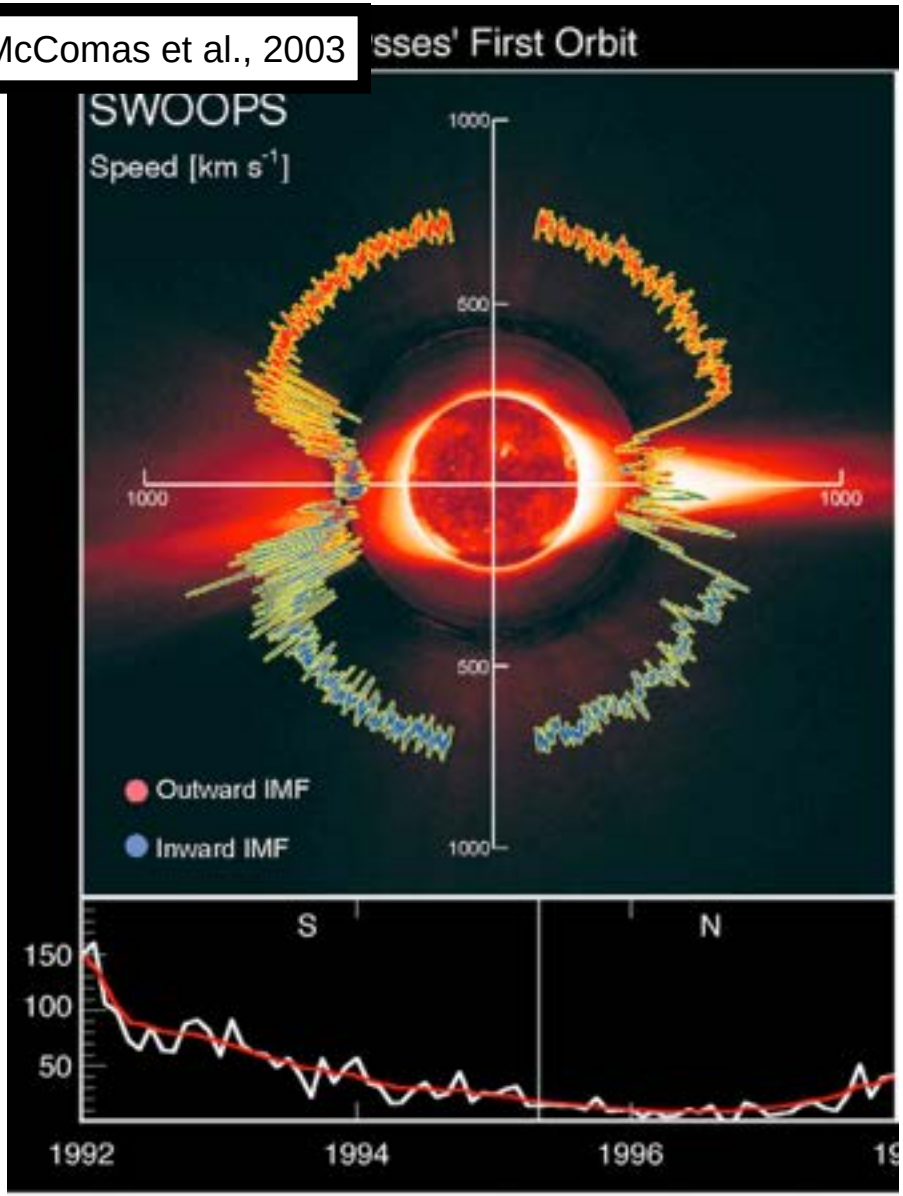


05-01481-68

**Figure 2-1**. Plots of solar wind speed as a function of heliographic latitude, illustrating the relation between the structure of the solar wind and coronal structure at solar minimum (left) and solar maximum (right). The baseline Solar Probe mission provides for two solar flybys, each at a different part of the solar cycle, so that measurements can be obtained at both the quiet and active phases of the cycle. (Ulysses SWOOPS solar

# Source of the solar wind: fast

**Fast wind:** coronal holes – consensus – this is Parker's "classical" solar wind.

Hassler et al., Science, 1999

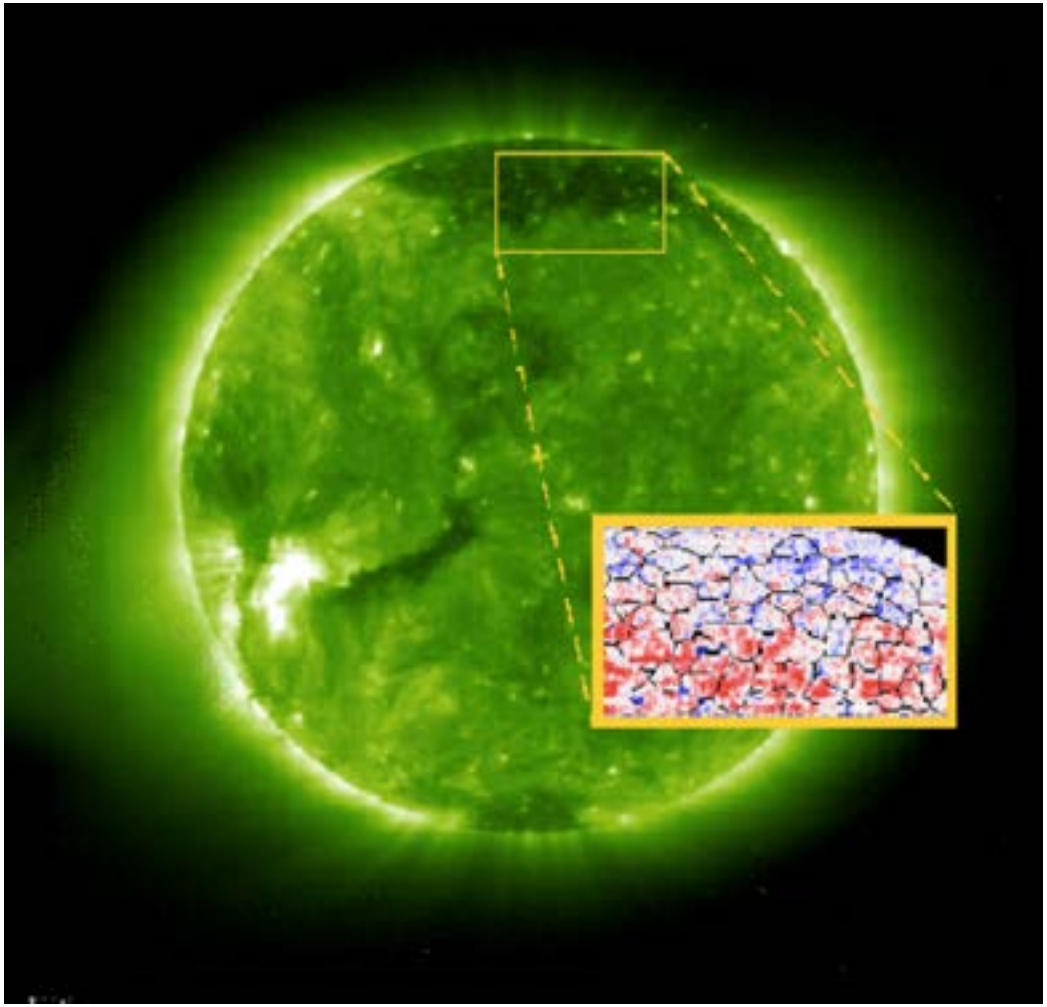

# Source of the solar wind: slow

**Slow wind:** edges of polar coronal holes, small, low-latitude CHs, streamer belt (tip of helmet streamers)… still quite controversial

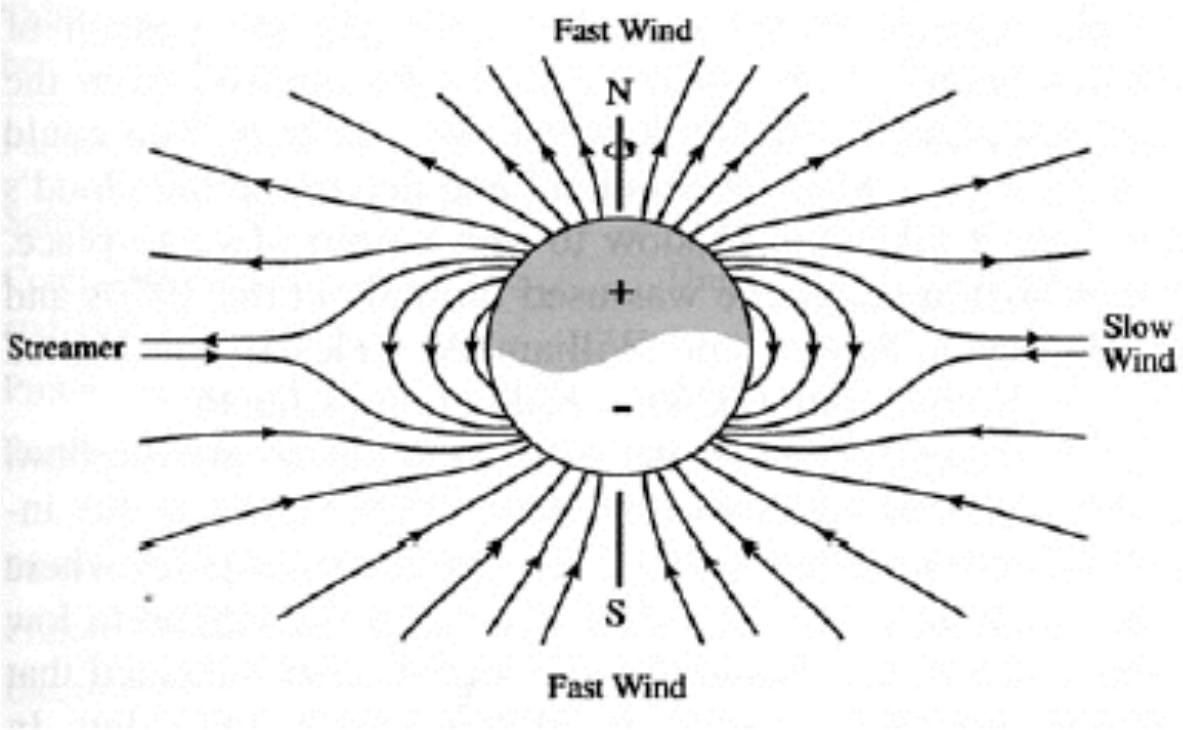

(van Driel-Gesztelyi et al., 2012)

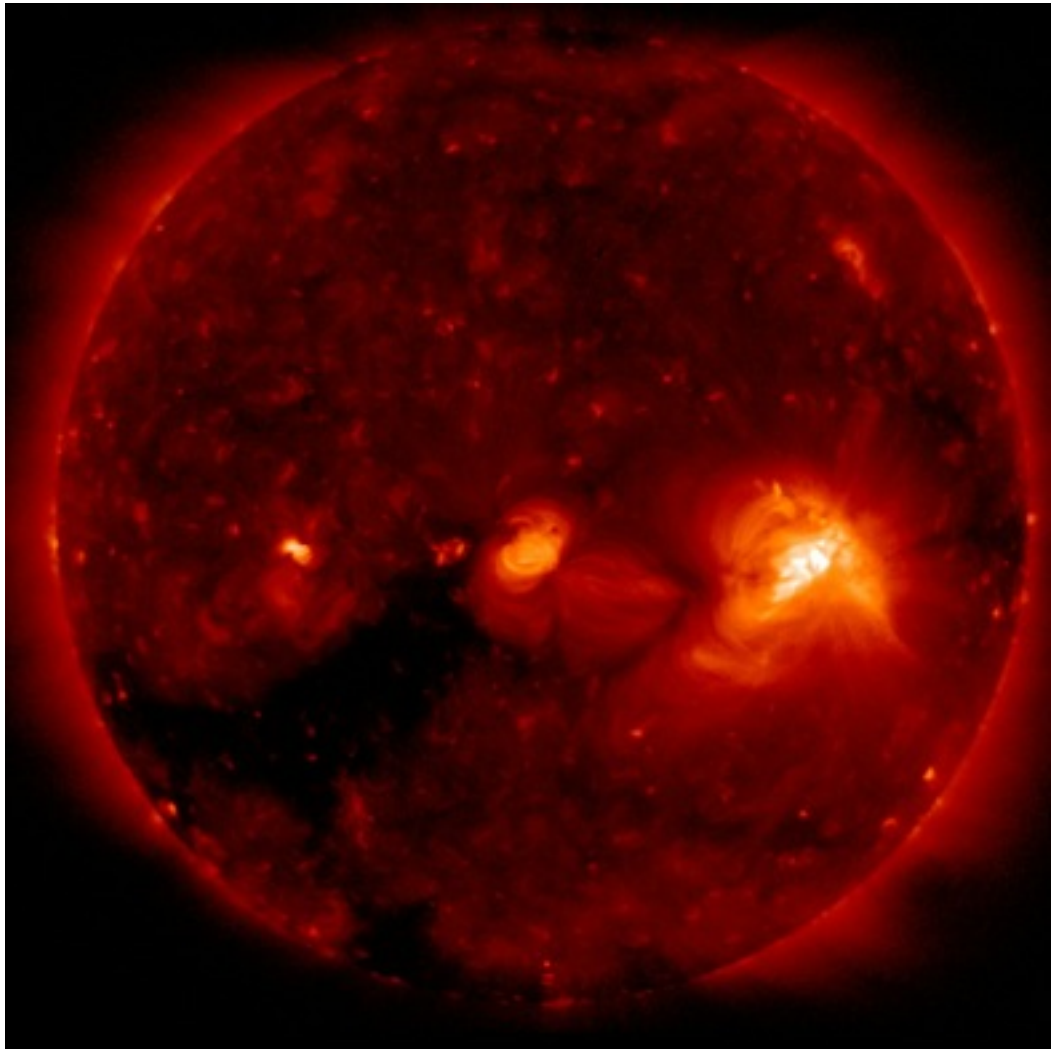

(van Driel-Gesztelyi et al., 2012)

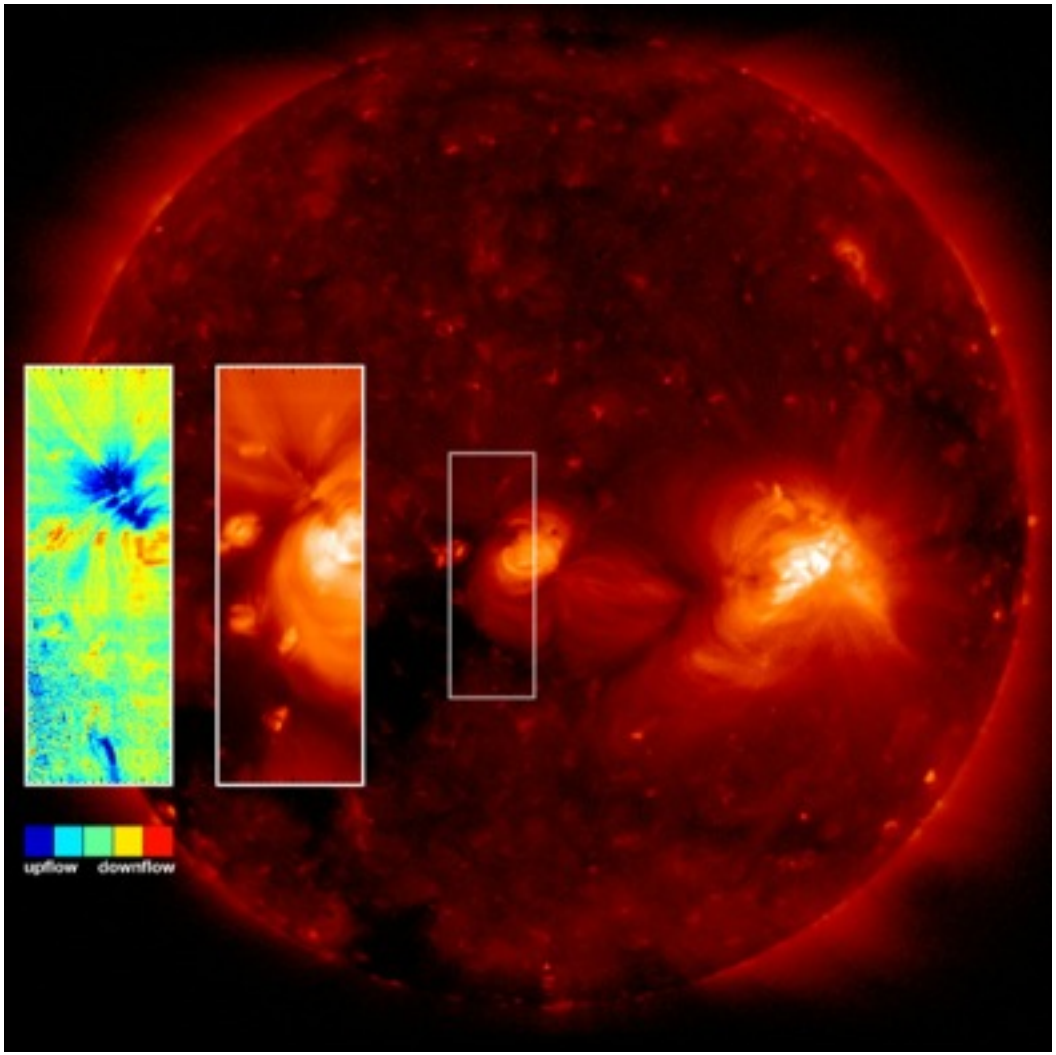

(van Driel-Gesztelyi et al., 2012)

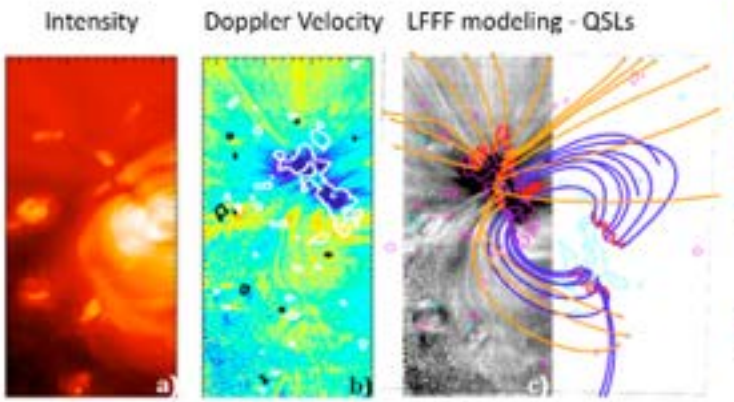


(A) Local LFFF extrapolations of AR2 - QSL locations

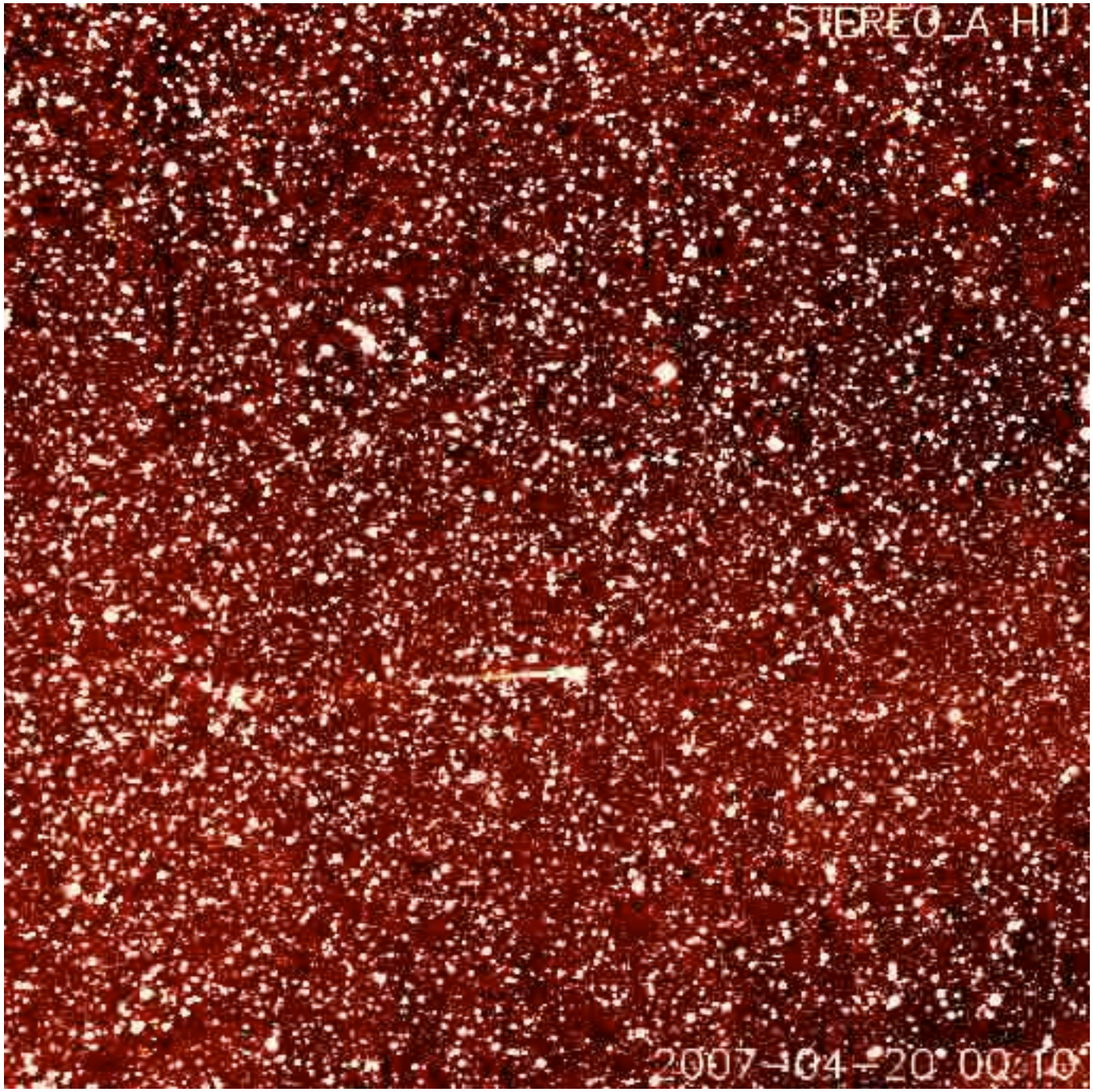
STEREO_A HI1
2007-04-20 00:10

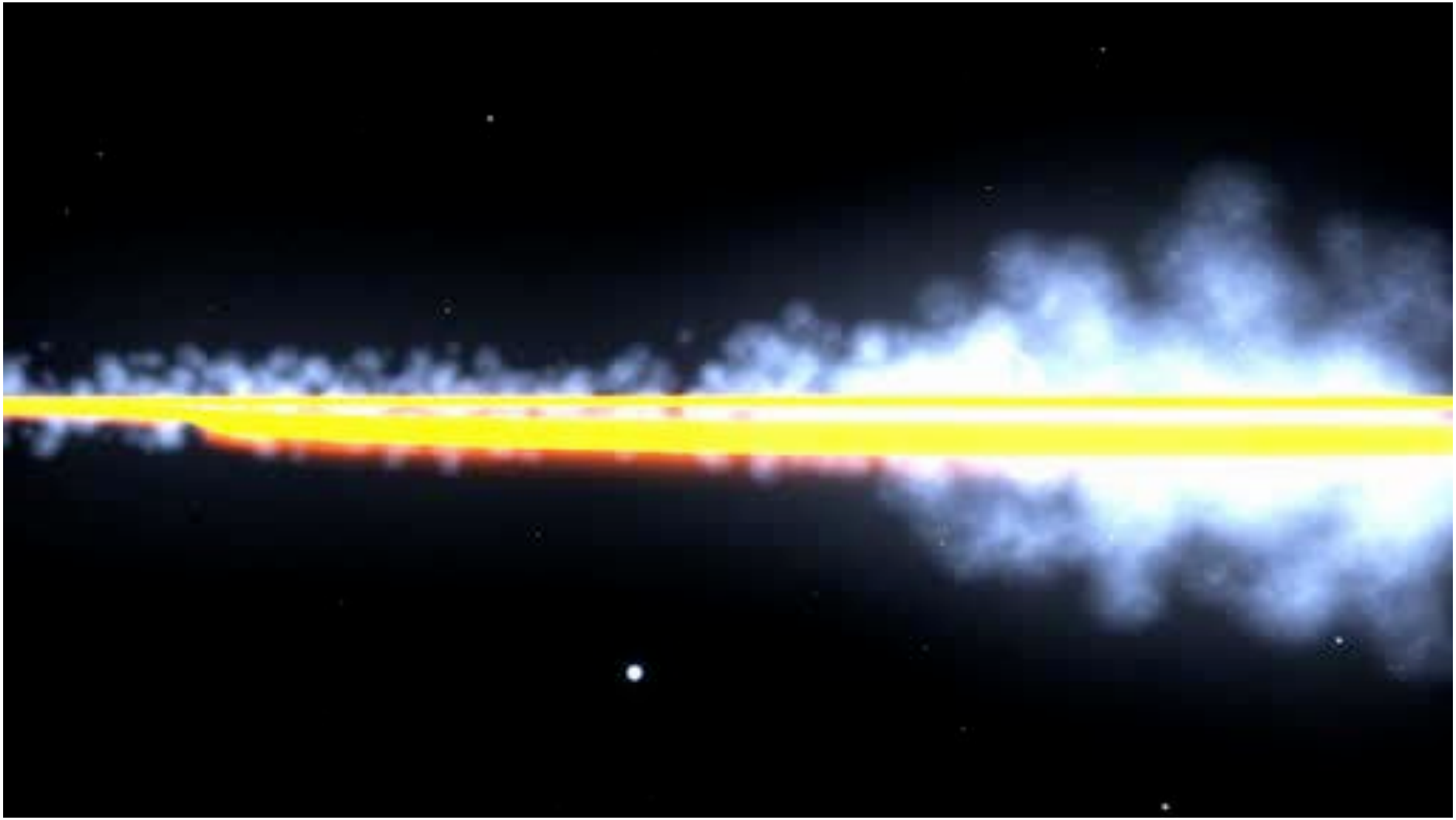

# The heliosphere

The solar wind creates a region ins space called the heliosphere.

- The point where the solar wind slows down → **termination shock**
- The point where the interstellar medium and solar wind pressures balance → **heliopause**
- The point where the interstellar medium, travelling in the opposite direction, slows down as it collides with the heliosphere → **bow shock**

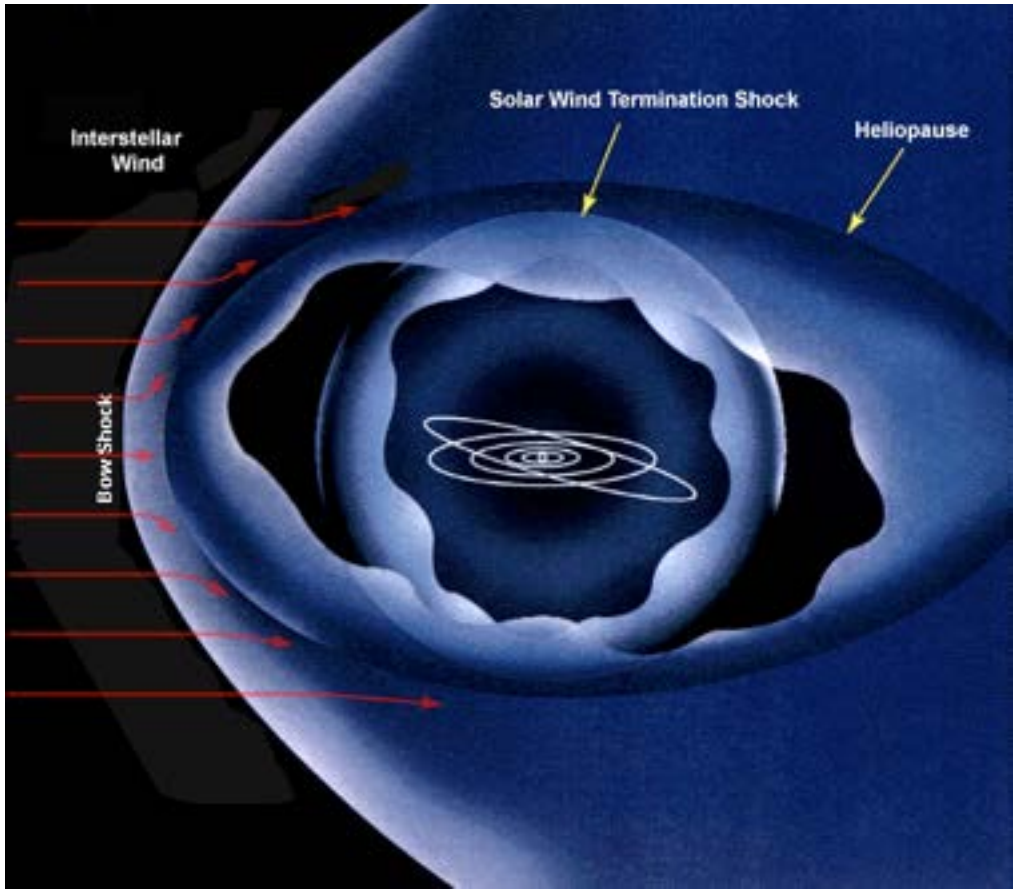


The distance to the termination shock can be estimated by determining the point at which the solar wind ram pressure is comparable to the ISM pressure.

- It was predicted to be greater than 100 AU, beyond the known major planets.
- Voyager 2 reached the termination shock in 2007 at a distance of 84 AU.

McComas et al., 2008

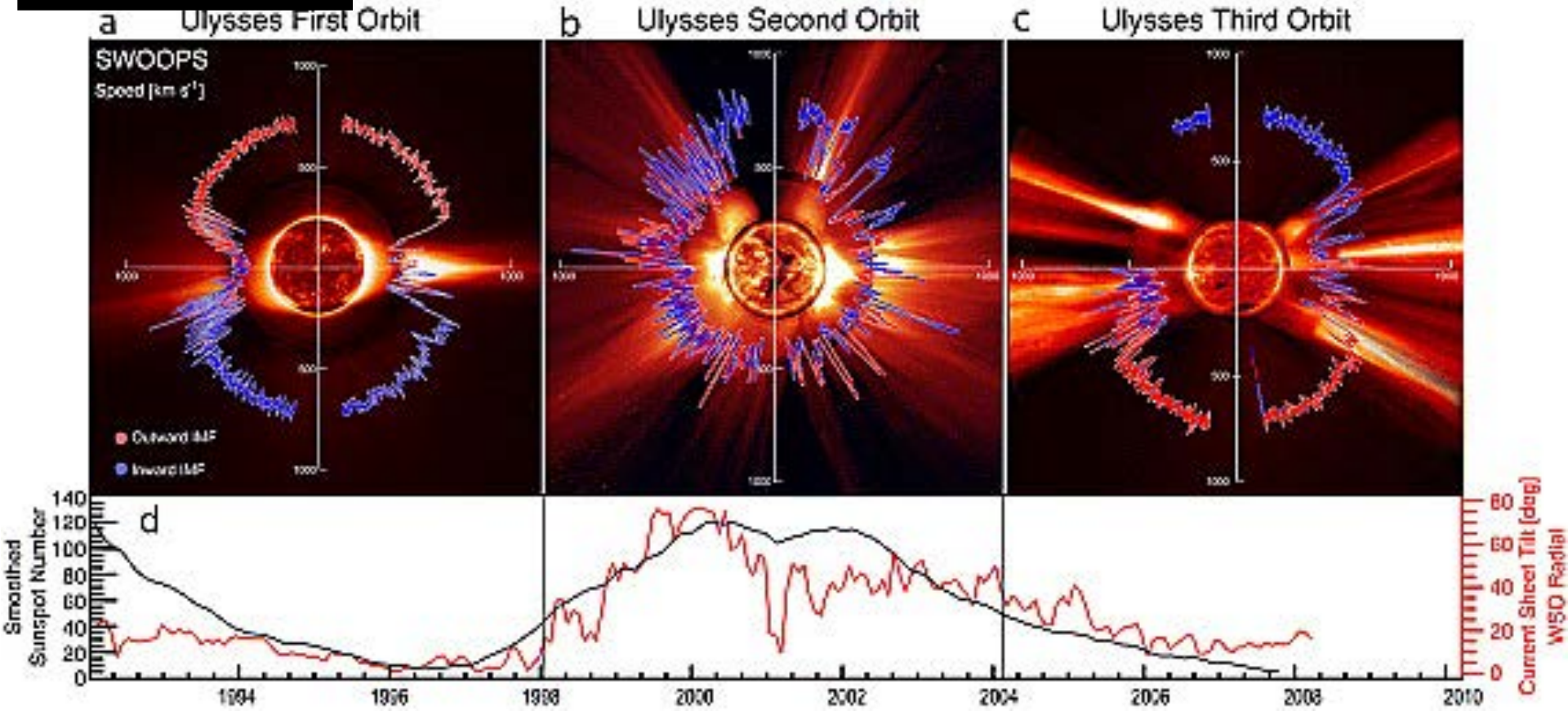

McComas et al., 2008

Observations during Ulysses' 3rd orbit showed that the **fast solar wind was slightly slower**, much l**ess dense**, **cooler**, and had less mass and momentum flux then during the 1st orbit (previous solar minimum). The significant long-term trend to lower dynamic pressures (was ~ 2nPa) meant that the heliosphere had to be shrinking and the heliopause moving inward toward the Voyager spacecraft.

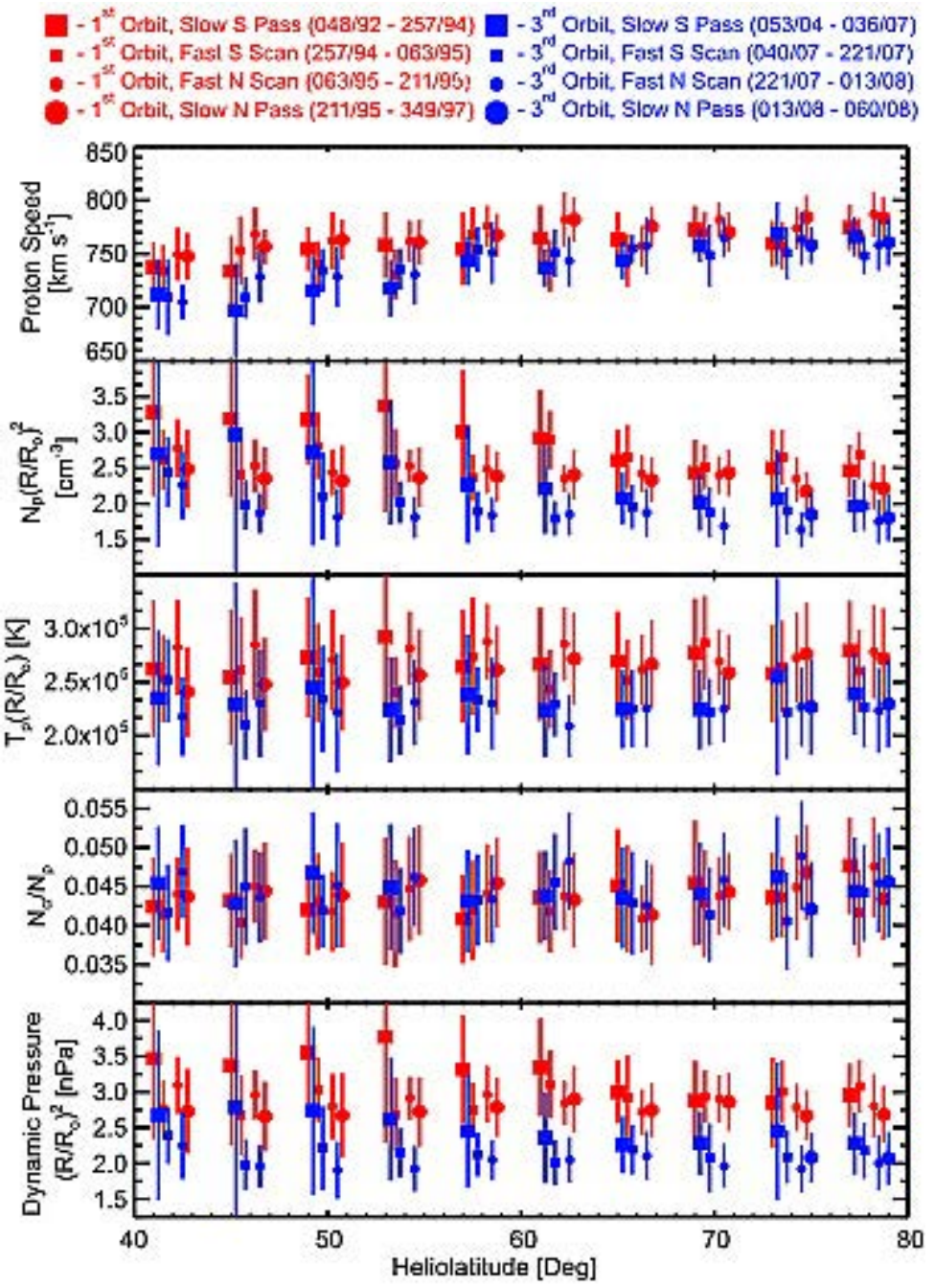

The Earth

The Sun

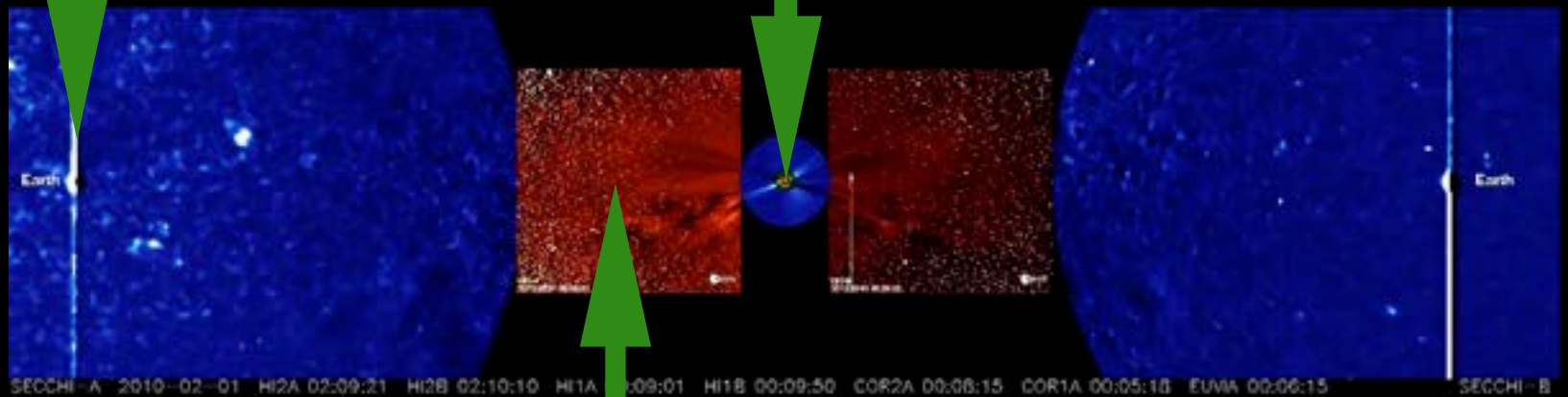


Solar Orbiter